Am J Physiol Heart Circ Physiol 294: H441–H448, 2008.
First published November 16, 2007; doi:10.1152/ajpheart.01021.2007.

Role of Cu,Zn-SOD in the synthesis of endogenous vasodilator hydrogen peroxide during reactive hyperemia in mouse mesenteric microcirculation in vivo

Toyotaka Yada,[1] Hiroaki Shimokawa,[2] Keiko Morikawa,[3] Aya Takaki,[2] Yoshiro Shinozaki,[4] Hidezo Mori,[5] Masami Goto,[1] Yasuo Ogasawara,[1] and Fumihiko Kajiya[1]

[1]Department of Medical Engineering and Systems Cardiology, Kawasaki Medical School, Kurashiki, Japan; [2]Department of Cardiovascular Medicine, Tohoku University Graduate School of Medicine, Sendai, Japan; [3]Department of Anesthesiology, Kyushu University Graduate School of Medical Sciences, Fukuoka, Japan; [4]Department of Physiology, Tokai University School of Medicine, Isehara, Japan; and [5]Department of Cardiac Physiology, National Cardiovascular Center Research Institute, Suita, Japan

Submitted 4 September 2007; accepted in final form 12 November 2007

Yada T, Shimokawa H, Morikawa K, Takaki A, Shinozaki Y, Mori H, Goto M, Ogasawara Y, Kajiya F. Role of Cu,Zn-SOD in the synthesis of endogenous vasodilator hydrogen peroxide during reactive hyperemia in mouse mesenteric microcirculation in vivo. *Am J Physiol Heart Circ Physiol* 294: H441–H448, 2008. First published November 16, 2007; doi:10.1152/ajpheart.01021.2007.—We have recently demonstrated that endothelium-derived hydrogen peroxide (H_2O_2) is an endothelium-derived hyperpolarizing factor and that endothelial Cu/Zn-superoxide dismutase (SOD) plays an important role in the synthesis of endogenous H_2O_2 in both animals and humans. We examined whether SOD plays a role in the synthesis of endogenous H_2O_2 during in vivo reactive hyperemia (RH), an important regulatory mechanism. Mesenteric arterioles from wild-type and Cu,Zn-SOD$^{-/-}$ mice were continuously observed by a pencil-type charge-coupled device (CCD) intravital microscope during RH (reperfusion after 20 and 60 s of mesenteric artery occlusion) in the cyclooxygenase blockade under the following four conditions: control, catalase alone, N^G-monomethyl-L-arginine (L-NMMA) alone, and L-NMMA + catalase. Vasodilatation during RH was significantly decreased by catalase or L-NMMA alone and was almost completely inhibited by L-NMMA + catalase in wild-type mice, whereas it was inhibited by L-NMMA and L-NMMA + catalase in the Cu,Zn-SOD$^{-/-}$ mice. RH-induced increase in blood flow after L-NMMA was significantly increased in the wild-type mice, whereas it was significantly reduced in the Cu,Zn-SOD$^{-/-}$ mice. In mesenteric arterioles of the Cu,Zn-SOD$^{-/-}$ mice, Tempol, an SOD mimetic, significantly increased the ACh-induced vasodilatation, and the enhancing effect of Tempol was decreased by catalase. Vascular H_2O_2 production by fluorescent microscopy in mesenteric arterioles after RH was significantly increased in response to ACh in wild-type mice but markedly impaired in Cu,Zn-SOD$^{-/-}$ mice. Endothelial Cu,Zn-SOD plays an important role in the synthesis of endogenous H_2O_2 that contributes to RH in mouse mesenteric smaller arterioles.

nitric oxide; endothelium-derived hyperpolarizing factor; arteriole; vasodilatation

THE ENDOTHELIUM SYNTHESIZES and releases endothelium-derived relaxing factors (EDRFs), including vasodilator prostaglandins, nitric oxide (NO), and as yet unidentified endothelium-derived hyperpolarizing factor (EDHF). Since the first reports on the existence of EDHFs (4, 8), several candidates for EDHF have been proposed (9), including cytochrome *P*-450 metabolites (2, 3), endothelium-derived K^+ channel (7), and electrical communications through gap junctions between endothelial cells and vascular smooth muscle cells (34). Matoba et al. (19a, 19b, 20) previously identified that endothelium-derived hydrogen peroxide (H_2O_2) is a primary EDHF in mesenteric arteries of mice, pigs, and humans. Morikawa et al. (24a, 25) subsequently confirmed that endothelial Cu/Zn-superoxide dismutase (SOD) plays an important role in synthesizing EDHF/H_2O_2 in mice and humans. Recently, our laboratory (41a, 42) confirmed that endogenous H_2O_2 plays an important role for autoregulation and protection against reperfusion injury in canine coronary microcirculation.

Reactive hyperemia (RH) is an important regulatory mechanism of the cardiovascular system in response to a temporal reduction in blood flow for which both mechanosensitive (e.g., myogenic and shear mediated) and metabolic regulatory processes may be involved (6, 14a, 28). For the RH response of canine coronary microcirculation, NO, ATP-sensitive K^+ channels, and adenosine may all be involved (11, 41). Shear stress plays a crucial role in modulating vascular tone by stimulating the release of EDRFs (8, 32), and all three EDRFs (PGI_2, NO, and EDHF) are involved in flow-induced vasodilatation (15, 18, 33, 44).

However, it remains to be examined whether endogenous H_2O_2 is involved in the vasodilator mechanism of RH and, if so, whether endothelial Cu,Zn-SOD plays a role in the synthesis of endogenous H_2O_2 during RH. The present study was thus designed to address these important issues in mice. Our laboratory (42, 44) previously reported that the contribution of EDHF to the vasodilatory mechanisms increases as the diameter of the vessel decreases. Thus, by employing a pencil-type charge-coupled device (CCD) intravital microscope with a high resolution, we focused on the arterioles with a diameter of <50 μm in vivo.

METHODS

The present study was approved by the Animal Care and Use Committee of Kawasaki Medical School and conformed to the guidelines on animal experiments of Kawasaki Medical School and *the*

Address for reprint requests and other correspondence: Toyotaka Yada, Dept. of Medical Engineering and Systems Cardiology, Kawasaki Medical School, 577 Matsushima, Kurashiki, Okayama 701-0192 Japan (e-mail: yada@me.kawasaki-m.ac.jp).

The costs of publication of this article were defrayed in part by the payment of page charges. The article must therefore be hereby marked "*advertisement*" in accordance with 18 U.S.C. Section 1734 solely to indicate this fact.

Guide for the Care and Use of Laboratory Animals published by the National Institutes of Health.

Animal preparation. Male Cu,Zn-SOD$^{-/-}$ and control mice (10–16 wk of age) derived from breeding pairs of heterozygous (Cu,Zn-SOD$^{+/-}$) mice (Jackson Laboratory, Bar Harbor, ME) were used (25). They were placed on a heating blanket to maintain body temperature at 37°C throughout the experiment. The animals were anesthetized with 1% inhalational anesthesia of isoflurane. After tracheal intubation, they were ventilated with a mixture of room air and oxygen by a ventilator. The abdomen was opened, and a 24-Fr catheter was inserted into the abdominal aorta to measure aortic pressure. Mesenteric arterioles were continuously observed by a pencil-type intravital microscope (Nihon Kohden, Tokyo, Japan) (13).

Measurements of diameter by pencil-type intravital microscope. Mesenteric arterioles were visualized using a pencil-type intravital microscope (13). The system was modified for the visualization of microcirculation from our previous needle-probe CCD videomicroscope system (40). The microscopic images were monitored and recorded on a digital videocassette recorder (Sony, Tokyo, Japan) every 33 ms (30 frames/s). The spatial resolution of a static image of this system is 0.5 μm for ×600 magnification. The field of view is 367 × 248 μm, and the focal depth is 50 μm.

Measurements of regional blood flow in mesenteric arteries. Regional blood flow in mesenteric arteries was measured by the nonradioactive microsphere (15 μm; Sekisui Plastic, Tokyo, Japan) technique at the end of the experiments, as previously described (24). Briefly, a bolus (50 μl) of the microspheres suspension (5 × 10^5 spheres; Ce and Ba) were injected into the abdominal aorta at baseline and 5 s after the reperfusion of the mesenteric artery with confirming changes of the blood flow of the mesenteric artery by a CCD intravital microscope and without inducing hemodynamic changes (14). Mice were euthanized, and the mesenterium was extracted. The X-ray fluorescence of the stable heavy elements was measured by a wavelength-dispersive spectrometer (model PW 1480; Phillips, Eindhoven, the Netherlands). The relative increase in blood flow of mesenterium [microsphere count/tissue weight (g)] during RH from baseline was calculated.

Detection of H_2O_2 and NO production in mesenteric microvessels. 2′,7′-Dichlorodihydrofluorescein diacetate (DCF-DA; Molecular Probes, Eugene, OR) and diaminorhodamine-4M AM (DAR; Daiichi Pure Chemicals, Tokyo, Japan) were used to detect H_2O_2 and NO production in mesenteric microvessels, respectively, as previously described (41a). Briefly, fresh and unfixed mesenteric tissue was cut into several blocks and immediately frozen in an optimal cutting temperature compound (Tissue-Tek; Sakura Fine Chemical, Tokyo, Japan). After washout of the mesenteric tissue with phosphate-buffered solution under a normal temperature, fluorescent images of the microvessels were obtained 3 min after application of acetylcholine (ACh) by using a fluorescence microscope (Olympus BX51) (41a). We defined the baseline fluorescent intensity as the response in the vascular endothelium just after the injection of NO or H_2O_2 fluorescent dye. The fluorescence data at baseline (both DCF-DA and DAR) were obtained after the RH.

Experimental protocol. We performed four protocols. First, mesenteric arterioles in wild-type and Cu,Zn-SOD$^{-/-}$ mice were continuously observed by a pencil-type intravital microscope during RH (reperfusion after 20 and 60 s of mesenteric artery occlusion) with cyclooxygenase blockade [indomethacin, 5 × 10^{-5} mol/l topical administration (ta)] with the following four conditions: control, catalase alone [1,500 U·min^{-1}·100 g body wt^{-1} intra-arterial administration (ia) polyethylene glycol-catalase, a specific decomposer of H_2O_2], NO synthase inhibitor alone (10^{-4} mol/l ta L-NMMA), and L-NMMA + catalase (17). In the presence of indomethacin and L-NMMA, microspheres were administered at baseline and 5 s after the reperfusion into the abdominal aorta by bolus injection because RH peaked within 20–60 s after release from 20- and 60-s occlusion (29). Maximal vascular diameter was measured within 20 and 60 s after the reperfusion. Second, ACh (10^{-7} to 10^{-5} mol/l ta)-induced endothelium-dependent vasodilatation was examined under the control conditions and in the presence of Tempol, a SOD mimetic 4-hydroxy-2,2,6,6-tetramethylpiperidine-*N*-oxyl (50 μg·min^{-1}·100 g body wt^{-1} ia) (17), and Tempol + catalase. In the combined infusion protocol (Tempol or Tempol + catalase) in the presence of cyclooxygenase blockade + L-NMMA, the combined infusion was performed simultaneously for 20 min, ACh was infused for 10 min, and the vascular diameter was measured. Third, sodium nitroprusside (SNP; 10^{-7} to 10^{-5} mol/l ta, each 10 min)-induced endothelium-independent vasodilatation was examined in wild-type and Cu,Zn-SOD$^{-/-}$ mice. Fourth, fresh and unfixed mesenteric tissue was then cut into several blocks and immediately frozen in optimal cutting temperature compound.

Statistical analysis. The results are expressed as means ± SE. Dose-response curves were analyzed by two-way ANOVA followed by the Scheffé's post hoc test for multiple comparisons. Vascular responses were analyzed by one-way ANOVA followed by the Scheffé's post hoc test for multiple comparisons. $P < 0.05$ was considered to be statistically significant.

RESULTS

Hemodynamics and blood gases during RH. Throughout the experiments, mean aortic pressure and heart rate were constant and comparable (Tables 1 and 2), and Po_2, Pco_2, and pH were maintained within the physiological ranges (>70 mmHg Po_2, 25–40 mmHg Pco_2, and pH 7.35–7.45). Baseline mesenteric

Table 1. *Hemodynamics during RH*

		Control		Catalase		L-NMMA		L-NMMA + Catalase	
	n	B	RH	B	RH	B	RH	B	RH
MBP, RH 20, mmHg									
WT	10	83±7	85±9	81±7	82±7	82±8	81±6	83±8	82±6
Cu/Zn-SOD$^{-/-}$	10	85±12	87±10	83±8	82±8	82±8	82±8	82±8	80±9
MBP, RH 60, mmHg									
WT	5	86±8	88±7	87±7	88±7	88±8	87±7	88±7	87±7
Cu/Zn-SOD$^{-/-}$	5	88±8	86±8	87±6	89±9	88±7	88±8	89±6	90±11
HR, RH 20, beats/min									
WT	10	346±14	348±14	335±15	333±17	315±15	310±17	330±18	330±18
Cu/Zn-SOD$^{-/-}$	10	364±27	354±22	350±18	351±15	355±15	340±17	355±15	335±17
HR, RH 60, beats/min									
WT	5	351±31	361±9	353±21	356±13	358±10	364±37	354±22	355±15
Cu/Zn-SOD$^{-/-}$	5	346±18	356±25	356±15	361±19	351±31	361±9	358±10	364±27

Values are means ± SE; *n*, number of rats. RH, reactive hyperemia; L-NMMA, N^G-monomethyl-L-arginine; B, baseline; MBP, mean blood pressure; HR, heart rate; WT, wild-type.

Table 2. *Hemodynamics during administration of ACh and SNP*

	n	Control			Tempol			Tempol + Catalase			SNP			
		B	ACh 10^{-7}	ACh 10^{-6}	ACh 10^{-5}	ACh 10^{-7}	ACh 10^{-6}	ACh 10^{-5}	ACh 10^{-7}	ACh 10^{-6}	ACh 10^{-5}	B	SNP 10^{-7}	SNP 10^{-6}	SNP 10^{-5}
MBP, mmHg															
WT	10	90±7	88±7	87±7	89±6	91±10	90±11	84±11	91±8	86±8	86±8	78±13	77±13	76±13	76±13
CuZn-SOD$^{-/-}$	10	93±11	92±10	94±10	97±10	98±16	97±15	99±15	91±8	91±8	88±8	81±8	77±10	75±11	74±11
HR, beats/min															
WT	10	361±9	340±17	340±17	340±17	342±24	336±25	336±25	320±19	330±27	330±27	370±57	364±37	351±31	351±31
CuZn-SOD$^{-/-}$	10	386±11	381±24	371±21	396±13	386±11	377±15	377±15	362±22	356±25	356±25	372±21	369±6	358±10	346±18

Values are means ± SE; *n*, number of rats. SNP, sodium nitroprusside; ACh, acetylcholine.

arteriolar diameter was comparable in the absence and presence of inhibitors under the four different experimental conditions (Tables 3 and 4). Those different inhibitors (L-NMMA, catalase, and Tempol) did not affect basal diameter.

Mesenteric vasodilatation during RH. We were able to observe EDHF-sensitive smaller arterioles (18–66 μm) by using a newly developed pencil-type CCD intravital microscope with a higher resolution. In the mesenteric arterioles of wild-type mice, vasodilatation during RH to 20- and 60-s arterial occlusion was decreased by catalase or L-NMMA alone and was almost completely inhibited by L-NMMA + catalase (Fig. 1). In contrast, in mesenteric arterioles of Cu,Zn-SOD$^{-/-}$ mice, vasodilatation during RH to 20- and 60-s arterial occlusion was decreased by catalase alone and was almost completely inhibited by L-NMMA alone or L-NMMA + catalase (Fig. 1). Blood flow measurement by microsphere technique showed that in the presence of indomethacin and L-NMMA, RH-induced increase in blood flow was 232 ± 4% (20 s) and 331 ± 4% (60 s) of baseline in control and was sensitive to catalase (137 ± 4%, 20 s; and 147 ± 17%, 60 s) in the wild-type mice, whereas in the Cu,Zn-SOD$^{-/-}$ mice, the vasodilator response was significantly reduced to 125 ± 19% (20 s) and 145 ± 23% (60 s) in control and was insensitive to catalase (120 ± 24%, 20 s; and 139 ± 19%, 60 s) (Fig. 2). With the longer occlusion of the mesenteric artery, the shear stimulus for H_2O_2 release was significantly increased in the control condition and was significantly decreased by catalase.

Endothelium-dependent vasodilatation. In mesenteric arterioles of wild-type mice, endothelium-dependent vasodilatation to ACh (10^{-7} to 10^{-5} mol/l in the presence of indomethacin and L-NMMA) was unchanged with Tempol but significantly inhibited by the addition of catalase (Fig. 3). In contrast, in the mesenteric arterioles of the Cu,Zn-SOD$^{-/-}$ mice, the response to ACh was significantly enhanced with Tempol, a response that was sensitive to the addition of catalase (Fig. 3).

Endothelium-independent vasodilatation. Endothelium-independent vasodilatation to SNP (10^{-7} to 10^{-5} mol/l in the presence of L-NMMA + catalase) was comparable between the two strains (Table 4).

Detection of H_2O_2 and NO production in the mesenteric artery. Fluorescent microscopy with DCF-DA showed that vascular H_2O_2 production in mesenteric arterioles was significantly increased in response to ACh in wild-type mice compared with baseline but markedly impaired in Cu,Zn-SOD$^{-/-}$ mice (Fig. 4). In contrast, vascular NO production in mesenteric arterioles, as assessed by DAR fluorescent intensity, was significantly increased in response to ACh in wild-type mice compared with baseline and was unaltered in Cu,Zn-SOD$^{-/-}$ mice (Fig. 5).

DISCUSSION

The novel finding of the present study with a newly developed pencil-type CCD intravital microscope in vivo is that Cu,Zn-SOD plays an important role in the synthesis of endogenous H_2O_2, which is substantially involved in the mechanisms of RH-induced vasodilatation in mouse mesenteric circulation.

Impaired EDHF-mediated vasodilatation in Cu,Zn-SOD$^{-/-}$ mice in vivo. Matoba et al. (19a, 20) have previously identified that endothelium-derived H_2O_2 is an EDHF in mouse and

Table 3. *Diameter change during RH*

	Control		Catalase		L-NMMA		L-NMMA + Catalase	
	B	RH	B	RH	B	RH	B	RH
RH 20, μm								
WT	36±4	49±4†	36±4	44±4†	36±3	42±3*	36±4	38±3
Cu/Zn-SOD$^{-/-}$	36±4	48±5†	36±4	42±5†	36±4	38±4	36±3	38±4
RH 60, μm								
WT	40±4	55±4†	40±4	51±4†	40±5	47±4*	39±4	41±4
Cu/Zn-SOD$^{-/-}$	40±3	56±4†	40±3	51±4†	39±4	42±3	40±5	42±3

Values are means ± SE; *n*, number of arterioles per animal. *$P < 0.01$ vs. B.

human mesenteric microvessels. Subsequently, our laboratory (42) and others (23) have confirmed that endogenous H_2O_2 exerts important vasodilator effects in canine coronary microcirculation in vivo and in isolated human coronary microvessels, respectively. H_2O_2 can be formed from superoxide anions derived from several sources in endothelial cells, including endothelial NO synthase (eNOS), cyclooxygenase, lipoxygenase, cytochrome *P*-450 enzymes, and reduced NADP [NAD(P)H] oxidases. Gupte et al. (10) demonstrated that cytosolic NADH redox and Cu,Zn-SOD activity have important roles in controlling the inhibitory effects of superoxide anions derived from NADH oxidase. Morikawa et al. (24a, 25) have also demonstrated that endothelial Cu,Zn-SOD plays an important role in the synthesis of H_2O_2 in mouse and human mesenteric arteries in vitro.

In the present study, catalase or L-NMMA alone significantly, but not completely, inhibited the RH-induced vasodilatation of mesenteric arterioles in wild-type mice in vivo, whereas L-NMMA + catalase markedly attenuated the remaining vasodilatation. In contrast, in Cu,Zn-SOD$^{-/-}$ mice, L-NMMA alone significantly decreased the vasodilatation and blood flow in response to 20- and 60-s arterial occlusion (Figs. 1 and 2). These results obtained using a pencil-type CCD intravital microscope indicate that H_2O_2 exerts important vasodilator effects on mesenteric smaller arterioles during RH and that Cu,Zn-SOD plays an important role in the synthesis of endogenous H_2O_2 during RH in vivo. Koller and Bagi (14a) showed that RH in rat isolated coronary arterioles was sensitive to pressure/stretch and flow/shear stress. Miura et al. (23) also showed the important role of endogenous H_2O_2 in flow-induced vasodilatation of human coronary arterioles. Koller and Bagi (14a) also suggested that H_2O_2 contributes to the development of the early peak phase of RH but not the duration of reactive vasodilatation, whereas NO prolongs the later phase of RH in rat isolated coronary arterioles, suggesting that H_2O_2 released endogenously within the vascular wall changes hemodynamic forces. In the present study, peak blood flow was significantly decreased after catalase (Fig. 2), suggesting that flow-induced vasodilatation during the early phase of RH is indeed mediated by H_2O_2 in mouse mesenteric arterioles in vivo.

Compensatory vasodilator mechanism between H_2O_2 and NO. It is well known that coronary vascular tone is regulated by the interactions among hemodynamic forces and several endogenous vasodilators, including NO, H_2O_2, and adenosine (41a, 42). Koller and Bagi (14a) demonstrated that mechanosensitive mechanisms were activated by changes in pressure and flow/shear stress during RH in isolated coronary arterioles. A superoxide anion is dismutated to H_2O_2 by manganese SOD (Mn-SOD, mitochondrial matrix) and Cu,Zn-SOD. H_2O_2 diffuses across the mitochondrial membrane to act on vascular smooth muscle (45). Tsunoda et al. (35) demonstrated that Mn-SOD augmented RH during 60-s canine coronary ischemia and reperfusion. H_2O_2 generated in the arteriolar smooth muscle could cause the response of activation of cGMP in rat skeletal muscle arterioles (38). Kitakaze et al. (12) indicated that the augmentation of reactive hyperemic flow caused by SOD is attributed to the enhanced release of adenosine in canine coronary circulation. These endogenous vasodilators may play an important role in causing the compensatory vasodilatation of coronary microvessels during myocardial ischemia.

In the present study, endothelium-dependent vasodilatation during RH (in the presence of L-NMMA) was almost completely inhibited by catalase in wild-type mice. In the Cu,Zn-SOD$^{-/-}$ mice, vasodilatation during RH remained under the control condition but was almost completely inhibited by L-NMMA (Fig. 1). The RH-induced increase in blood flow (in the presence of indomethacin and L-NMMA) was significantly inhibited by catalase in the wild-type mice but not in Cu,Zn-SOD$^{-/-}$ mice (Fig. 2). RH-induced increase in blood flow (in the presence of indomethacin and L-NMMA) remained in Cu,Zn-SOD$^{-/-}$ mice (Fig. 2). H_2O_2 may compensate for the loss of action of NO. H_2O_2 produced by SOD other than Cu,Zn-SOD may compensate for the loss of action of Cu,Zn-SOD-derived H_2O_2.

Table 4. *Diameter change during administration of ACh and SNP*

	ACh				SNP			
	B	ACh 10^{-7}	ACh 10^{-6}	ACh 10^{-5}	B	SNP 10^{-7}	SNP 10^{-6}	SNP 10^{-5}
WT, μm	36±3	41±3*	45±3†	49±4†	35±4	39±4*	43±5†	46±5†
Cu/Zn-SOD$^{-/-}$, μm	36±4	38±4	41±4*	44±4†	34±4	38±4*	41±4†	44±4†

Values are means ± SE; *n*, number of arterioles per animal. *$P < 0.05$; †$P < 0.01$ vs. B.

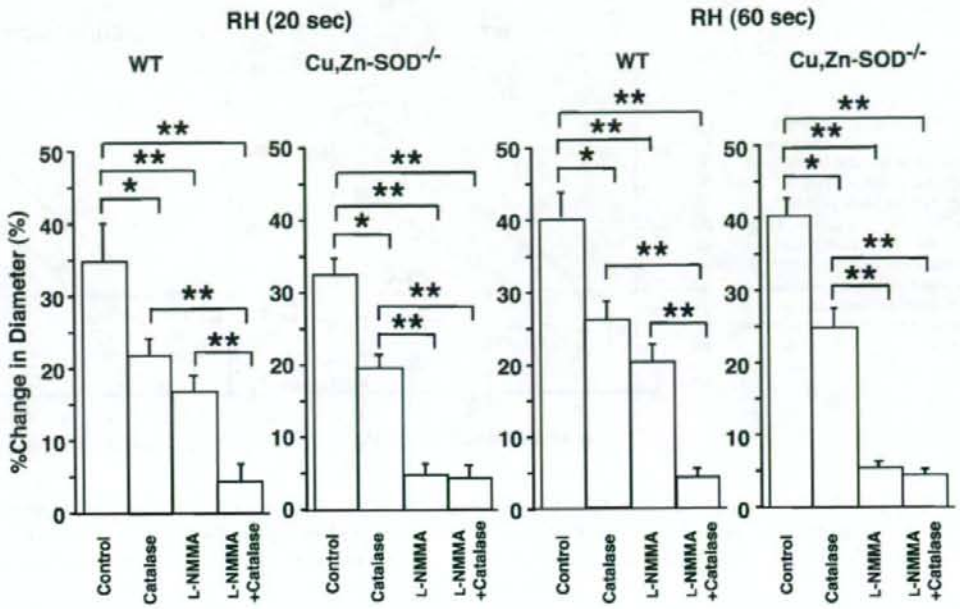

Fig. 1. Mesenteric vasodilatation during reactive hyperemia (RH). In the wild-type (WT) mice, vasodilatation during RH was inhibited by catalase or N^G-monomethyl-L-arginine (L-NMMA) and further inhibited by L-NMMA + catalase. In the Cu,Zn-SOD$^{-/-}$ mice (Cu,Zn-SOD$^{-/-}$), vasodilatation during RH was inhibited by catalase and markedly inhibited by L-NMMA, and the remaining response was not inhibited by catalase. The number of arterioles per animals used was 10/5 for each group. $*P < 0.05$; $**P < 0.01$.

Improvement of ACh-induced vasodilatation by Tempol in Cu,Zn-SOD$^{-/-}$ mice. It was previously reported that Tempol, a cell membrane-permeable SOD mimetic 4-hydroxy-2,2,6,6-tetramethylpiperidine-*N*-oxyl, decreased oxidative stress in the spontaneously hypertensive rat (31). In the present study, Tempol significantly improved the ACh-induced vasodilatation in Cu,Zn-SOD$^{-/-}$ mice, whereas catalase abolished the beneficial effect of Tempol (Fig. 3), indicating that the effect of Tempol was mediated by endogenous H_2O_2 in vivo. In contrast, Tempol had no enhancing effect on the ACh-induced vasodilatation in control mice (Fig. 3), suggesting that a sufficient amount of SOD is present in this strain. In Cu,Zn-SOD$^{-/-}$ mice, L-NMMA did not abolish the ACh-induced vasodilation, and the DCF-DA stain showed remaining fluorescent intensity (Fig. 4). Thus the residual vasodilatation could be caused by the following possible mechanisms. First, NO may also be synthesized in a nonenzymatic manner (27). Nonenzymatic synthesis of NO could occur in the presence of NADPH, glutathione, and L-cysteine, etc., opposing the effects of NOS inhibition (27). Second, the effects of L-NMMA may be limited since it is known that L-NMMA does not abolish NO production (1). H_2O_2 produced from vascular smooth muscle cells and other tissues may also contribute to the residual vasodilation (5, 30). Third, the contribution of other proposed

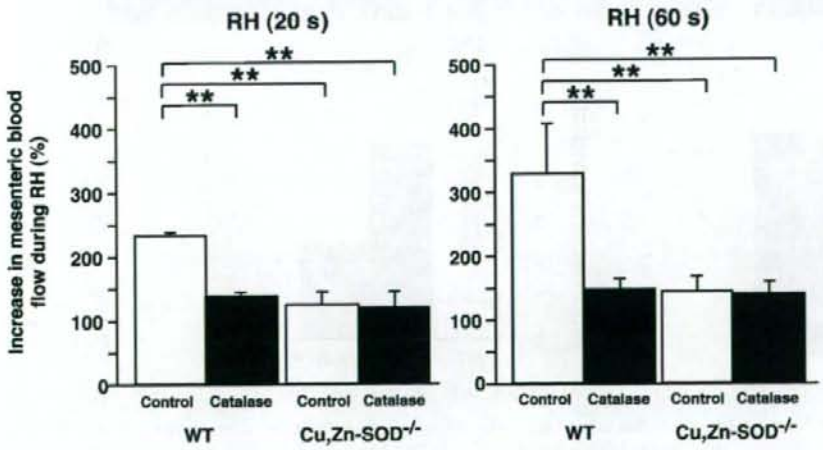

Fig. 2. The increase in mesenteric blood flow during RH. In the presence of indomethacin and L-NMMA, RH-induced increase in blood flow was sensitive to catalase in the WT mice, whereas in the Cu,Zn-SOD$^{-/-}$, the vasodilation was significantly reduced in control and was insensitive to catalase. The number of animals used was 5 for each group. $**P < 0.01$.

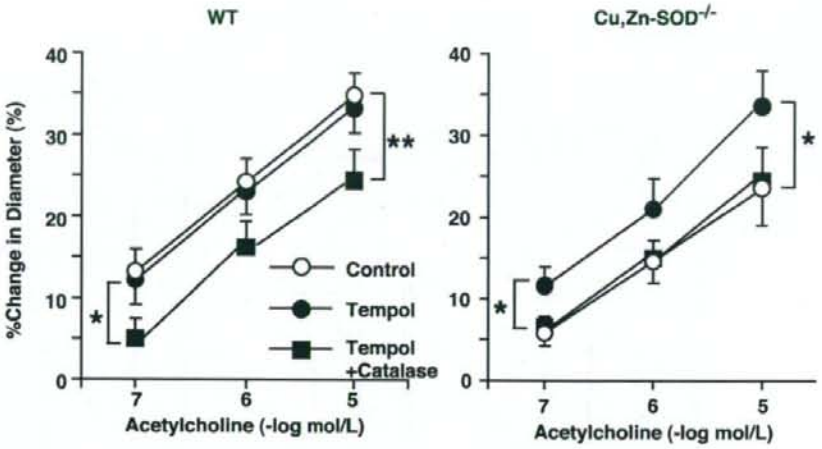

Fig. 3. Endothelium-dependent relaxations to ACh. In the WT mice, endothelium-dependent vasodilatation to ACh (in the presence of indomethacin and L-NMMA) was unchanged with Tempol but significantly inhibited by the addition of catalase. In the Cu,Zn-SOD$^{-/-}$, the vasodilation was significantly enhanced with Tempol, where the response was sensitive to the addition of catalase. The number of arterioles per animals used was 10/5 for each group. *P < 0.05; **P < 0.01.

EDHF candidates, such as P-450 metabolites (2, 3) and potassium ion (7), may contribute to the residual vasodilatation. Although RH and ACh have different mechanisms of vasodilator effects, they also share the same flow-induced vasodilator mechanism.

Endothelium-independent vasodilatation in Cu,Zn-SOD$^{-/-}$ mice. Microvascular dysfunction in hypercholesterolemic rats was confined to the endothelium because the dilator response to SNP and adenosine was unchanged (37). In the present study, endothelium-independent vasodilatation in response to SNP was comparable between the two genotypes, suggesting that vasodilatation properties of vascular smooth muscle cells were preserved in the Cu,Zn-SOD$^{-/-}$ mice in vivo.

Detection of vascular H_2O_2 and NO production. Our laboratory (41a) has recently demonstrated that vascular production of H_2O_2 and NO after ischemia-reperfusion is enhanced in small coronary arteries and arterioles in vivo, respectively. It was previously shown that a ACh-induced increase in fluorescence intensity in endothelial cells of the mesenteric artery is significantly reduced in Cu,Zn-SOD$^{-/-}$ mice (25). In the present study, vascular H_2O_2 production, as assessed by DCF-DA fluorescent intensity in mesenteric arterioles, was markedly impaired

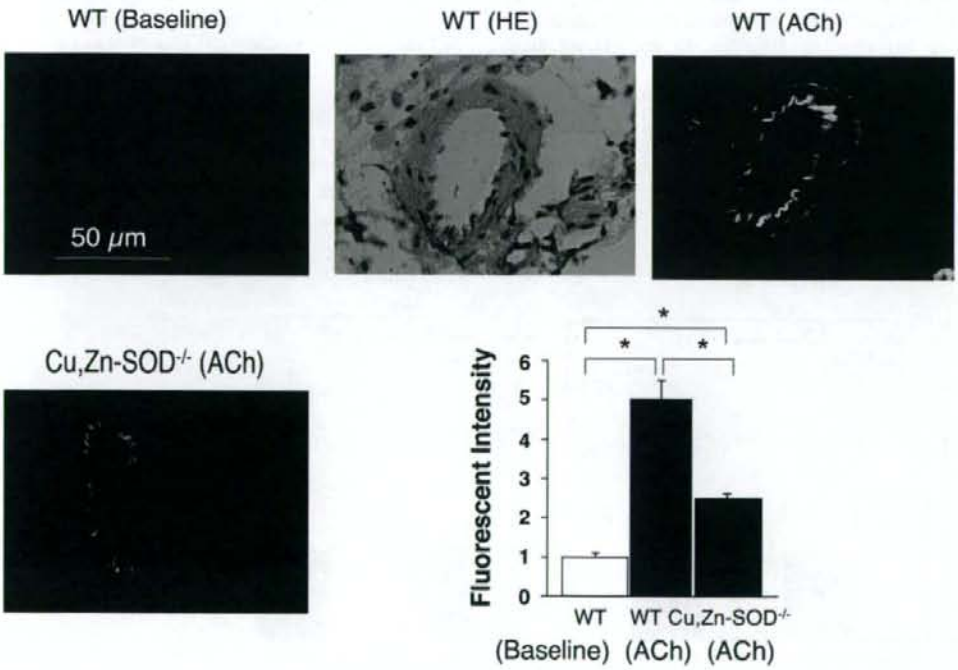

Fig. 4. Detection of vascular H_2O_2 production. Vascular H_2O_2 production in mesenteric arterioles was significantly increased in response to ACh in WT mice but markedly impaired in Cu,Zn-SOD$^{-/-}$. The number of arterioles per animals used was 10/5 for each group. *P < 0.05. HE, Hematoxylin eosin.

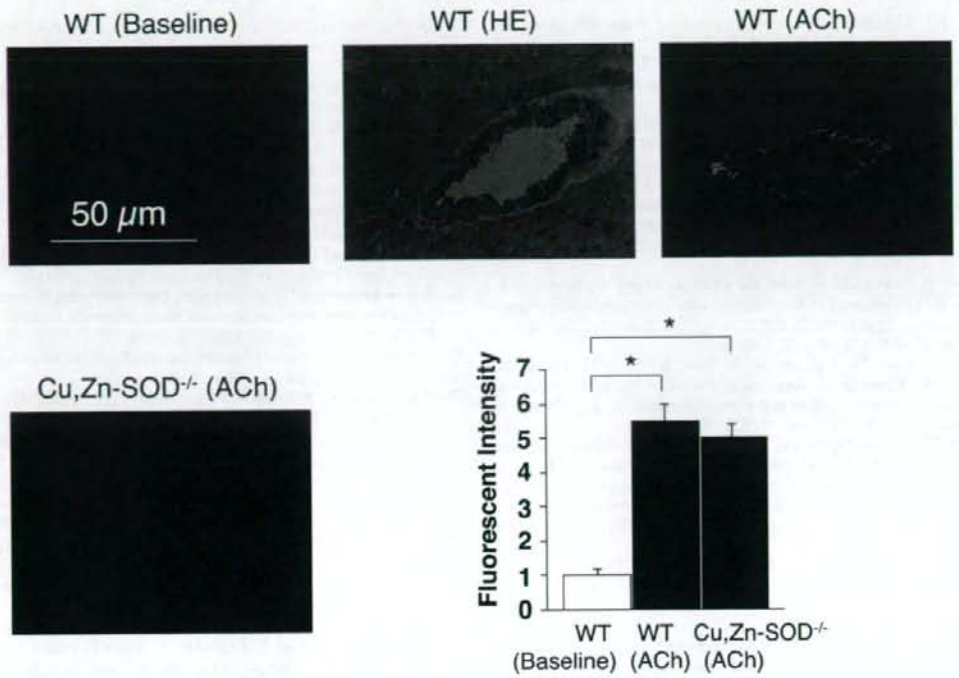

Fig. 5. Detection of vascular nitric oxide (NO) production. Vascular NO production in mesenteric arterioles was significantly increased in response to ACh in WT mice and unaltered in Cu,Zn-SOD$^{-/-}$. The number of arterioles per animals used was 10/5 for each group. *$P < 0.05$.

in Cu,Zn-SOD$^{-/-}$ mice (Fig. 4). These findings indicate that endothelial production of H_2O_2 is significantly impaired in Cu,Zn-SOD$^{-/-}$ mice, confirming the importance of the enzyme in endothelial synthesis of H_2O_2.

In the previous study by Morikawa et al. (25), eNOS protein expression was comparable between Cu,Zn-SOD$^{-/-}$ and wild-type mice. In the present study, vascular NO production in small mesenteric artery was unaltered in Cu,Zn-SOD$^{-/-}$ mice compared with wild-type mice (Fig. 5). NO could compensate for the loss of action of H_2O_2, although there are still many uncertainties about the local cellular dynamics of superoxide anions and NO.

Study limitations. Several limitations should be mentioned for the present study. First, we estimated blood flow in the mesenteric circulation using microspheres. We were unable to calculate the absolute values of local blood flow or shear stress because of the methodological limitations. However, since the flow measurement with microspheres was performed at the end of the experiments, it should not have influenced other results. Second, we used Cu,Zn-SOD$^{-/-}$ mice in the present study, where unknown compensatory mechanisms may be operative, and we were unable to elucidate the mechanism(s) for the remaining EDHF-mediated responses in those mice.

Clinical implications. RH is an important regulatory mechanism of the cardiovascular system, reflecting the flow reserve in response to a brief period of cessation of flow. An impaired flow reserve in resistance vessels is a hallmark of microvascular dysfunction with coronary risk factors. Hypertension is associated with structural alterations in the microcirculation and a reduced endothelium-dependent dilation in conduit arteries (19). It is well known that abnormality in Cu,Zn-SOD is noted in several diseases, including hypertension and diabetes mellitus (36, 39).

In conclusion, endogenous H_2O_2 exerts important vasodilator effects of mesenteric smaller arterioles during RH, especially at the low level of NO, and that Cu,Zn-SOD plays an important role in the synthesis of endogenous H_2O_2 during RH in vivo.

GRANTS

This work was supported in part by the Japanese Ministry of Education, Science, Sports, Culture, and Technology (Tokyo, Japan) Grants 16209027 (to H. Shimokawa), 16300164, and 19300167 (to T. Yada), the Program for Promotion of Fundamental Studies in Health Sciences of the Organization for Pharmaceutical Safety and Research of Japan (to H. Shimokawa), and Takeda Science Foundation 2002 (to T. Yada).

REFERENCES

1. **Amezcua JL, Palmer RM, de Souza BM, Moncada S.** Nitric oxide synthesized from L-arginine regulates vascular tone in the coronary circulation of the rabbit. *Br J Pharmacol* 97: 1119–1124, 1989.
2. **Bauersachs J, Hecker M, Busse R.** Display of the characteristics of endothelium-derived hyperpolarizing factor by a cytochrome P450-derived arachidonic acid metabolite in the coronary microcirculation. *Br J Pharmacol* 113: 1548–1553, 1994.
3. **Campbell WB, Gebremedhin D, Pratt PF, Harder DR.** Identification of epoxyeicosatrienoic acids as an endothelium-derived hyperpolarizing factor. *Circ Res* 78: 415–423, 1996.
4. **Chen G, Suzuki H, Weston AH.** Acetylcholine releases endothelium-derived hyperpolarizing factor and EDRF from blood vessels. *Br J Pharmacol* 95: 1165–1174, 1988.
5. **Chen Y, Pearlman A, Luo Z, Wilcox CS.** Hydrogen peroxide mediates a transient vasorelaxation with Tempol during oxidative stress. *Am J Physiol Heart Circ Physiol* 293: H2085–H2092, 2007.

6. **Coffman JD, Gregg DE.** Reactive hyperemia characteristics of the myocardium. *Am J Physiol* 199: 1143–1149, 1960.
7. **Edwards G, Dora KA, Gardener MJ, Garland CJ, Weston AH.** K^+ is an endothelium-derived hyperpolarizing factor in rat arteries. *Nature* 396: 269–272, 1998.
8. **Feletou M, Vanhoutte PM.** Endothelium-dependent hyperpolarization of canine smooth muscle. *Br J Pharmacol* 93: 515–524, 1988.
9. **Feletou M, Vanhoutte PM.** Endothelium-derived hyperpolarizing factor: where are we now? *Arterioscler Thromb Vasc Biol* 26: 1215–1225, 2006.
10. **Gupte SA, Rupawalla T, Mohazzab-H KM, Wolin MS.** Regulation of NO-elicited pulmonary artery relaxation and guanylate cyclase activation by NADH oxidase and SOD. *Am J Physiol Heart Circ Physiol* 276: H1535–H1542, 1999.
11. **Kanatsuka H, Sekiguchi N, Sato K, Akai K, Wang Y, Komaru T, Ashikawa K, Takishima T.** Microvascular sites and mechanisms responsible for reactive hyperemia in the coronary circulation of the beating canine heart. *Circ Res* 71: 912–922, 1992.
12. **Kitakaze M, Hori M, Takashima S, Iwai K, Sato H, Inoue M, Kitabatake A, Kamada T.** Superoxide dismutase enhances ischemia-induced reactive hyperemic flow and adenosine release in dogs. A role of 5′-nucleotidase activity. *Circ Res* 71: 558–566, 1992.
13. **Kiyooka T, Hiramatsu O, Shigeto F, Nakamoto H, Tachibana H, Yada T, Ogasawara Y, Kajiya M, Morimoto T, Morizane Y, Mohri S, Shimizu J, Ohe T, Kajiya F.** Direct observation of epicardial coronary capillary hemodynamics during reactive hyperemia and during adenosine administration by intravital video microscopy. *Am J Physiol Heart Circ Physiol* 288: H1437–H1443, 2005.
14. **Kobayashi N, Kobayashi K, Kouno K, Horinaka S, Yagi S.** Effects of intra-atrial injection of colored microspheres on systemic hemodynamics and regional blood flow in rats. *Am J Physiol Heart Circ Physiol* 266: H1910–H1917, 1994.

14a. **Koller A, Bagi Z.** Nitric oxide and H_2O_2 contribute to reactive dilation of isolated coronary arterioles. *Am J Physiol Heart Circ Physiol* 287: H2461–H2467, 2004.

15. **Koller A, Sun D, Kaley G.** Role of shear stress and endothelial prostaglandins in flow- and viscosity-induced dilation of arterioles in vitro. *Circ Res* 72: 1276–1284, 1993.
17. **Kopkan L, Castillo A, Navar LG, Majid DS.** Enhanced superoxide generation modulates renal function in ANG II-induced hypertensive rats. *Am J Physiol Renal Physiol* 290: F80–F86, 2006.
18. **Kuo L, Davis MJ, Chilian WM.** Endothelium-dependent, flow-induced dilation of isolated coronary arterioles. *Am J Physiol Heart Circ Physiol* 259: H1063–H1070, 1990.
19. **Lauer T, Heiss C, Preik M, Balzer J, Hafner D, Strauer BE, Kelm M.** Reduction of peripheral flow reserve impairs endothelial function in conduit arteries of patients with essential hypertension. *J Hypertens* 23: 563–569, 2005.

19a. **Matoba T, Shimokawa H, Kubota H, Morikawa K, Fujiki T, Kunihiro I, Mukai Y, Hirakawa Y, Takeshita A.** Hydrogen peroxide is an endothelium-derived hyperpolarizing factor in human mesenteric arteries. *Biochem Biophys Res Commun* 290: 909–913, 2002.

19b. **Matoba T, Shimokawa H, Morikawa K, Kubota H, Kunihiro I, Urakami-Harasawa L, Mukai Y, Hirakawa Y, Akaike T, Takeshita A.** Electron spin resonance detection of hydrogen peroxide as an endothelium-derived hyperpolarizing factor in porcine coronary microvessels. *Arterioscler Thromb Vasc Biol* 23: 1224–1230, 2003.

20. **Matoba T, Shimokawa H, Nakashima M, Hirakawa Y, Mukai Y, Hirano K, Kanaide H, Takeshita A.** Hydrogen peroxide is an endothelium-derived hyperpolarizing factor in mice. *J Clin Invest* 106: 1521–1530, 2000.
23. **Miura H, Bosnjak JJ, Ning G, Saito T, Miura M, Gutterman DD.** Role for hydrogen peroxide in flow-induced dilation of human coronary arterioles. *Circ Res* 92: e31–e40, 2003.
24. **Mori H, Haruyama S, Shinozaki Y, Okino H, Iida A, Takanashi R, Sakuma I, Husseini WK, Payne BD, Hoffman JI.** New nonradioactive microspheres and more sensitive X-ray fluorescence to measure regional blood flow. *Am J Physiol Heart Circ Physiol* 263: H1946–H1957, 1992.

24a. **Morikawa K, Fujiki T, Matoba T, Kubota H, Hatanaka M, Takahashi S, Shimokawa H.** Important role of superoxide dismutase in EDHF-mediated responses of human mesenteric arteries. *J Cardiovasc Pharmacol* 44: 552–556, 2004.

25. **Morikawa K, Shimokawa H, Matoba T, Kubota H, Akaike T, Talukder MA, Hatanaka M, Fujiki T, Maeda H, Takahashi S, Takeshita A.** Pivotal role of Cu,Zn-superoxide dismutase in endothelium-dependent hyperpolarization. *J Clin Invest* 112: 1871–1879, 2003.
27. **Moroz LL, Norby SW, Cruz L, Sweedler JV, Gillette R, Clarkson RB.** Non-enzymatic production of nitric oxide (NO) from NO synthase inhibitors. *Biochem Biophys Res Commun* 253: 571–576, 1998.
28. **Olsson RA.** Myocardial reactive hyperemia. *Circ Res* 37: 263–270, 1975.
29. **Pawlik WW, Obuchowicz R, Pawlik MW, Sendur R, Biernat J, Brzozowski T, Konturek SJ.** Histamine H_3 receptors modulate reactive hyperemia in rat gut. *J Physiol Pharmacol* 55: 651–661, 2004.
30. **Saitoh S, Zhang C, Tune JD, Potter B, Kiyooka T, Rogers PA, Knudson JD, Dick GM, Swafford A, Chilian WM.** Hydrogen peroxide: a feed-forward dilator that couples myocardial metabolism to coronary blood flow. *Arterioscler Thromb Vasc Biol* 26: 2614–2621, 2006.
31. **Schnackenberg CG, Wilcox CS.** Two-week administration of Tempol attenuates both hypertension and renal excretion of 8-Iso prostaglandin F_{2alpha}. *Hypertension* 33: 424–428, 1999.
32. **Shimokawa H.** Primary endothelial dysfunction: atherosclerosis. *J Mol Cell Cardiol* 31: 23–37, 1999.
33. **Takamura Y, Shimokawa H, Zhao H, Igarashi H, Egashira K, Takeshita A.** Important role of endothelium-derived hyperpolarizing factor in shear stress-induced endothelium-dependent relaxations in the rat mesenteric artery. *J Cardiovasc Pharmacol* 34: 381–387, 1999.
34. **Taylor HJ, Chaytor AT, Evance WH, Griffith TM.** Inhibition of the gap junctional component of endothelium-dependent relaxations in rabbit iliac artery by 18-alpha glycyrrhetinic acid. *Br J Pharmacol* 125: 1–3, 1998.
35. **Tsunoda R, Okumura K, Ishizaka H, Matsunaga T, Tabuchi T, Tayama S, Yasue H.** Enhancement of myocardial reactive hyperemia with manganese-superoxide dismutase: role of endothelium-derived nitric oxide. *Cardiovasc Res* 31: 537–545, 1996.
36. **Uchimura K, Nagasaka A, Hayashi R, Makino M, Nagata M, Kakizawa H, Kobayashi T, Fujiwara K, Kato T, Iwase K, Shinohara R, Kato K, Itoh M.** Changes in superoxide dismutase activities and concentrations and myeloperoxidase activities in leukocytes from patients with diabetes mellitus. *J Diabetes Complications* 13: 264–270, 1999.
37. **VanTeeffelen JW, Constantinescu AA, Vink H, Spaan JA.** Hypercholesterolemia impairs reactive hyperemic vasodilation of 2A but not 3A arterioles in mouse cremaster muscle. *Am J Physiol Heart Circ Physiol* 289: H447–H454, 2005.
38. **Wolin MS, Rodenburg JM, Messina EJ, Kaley G.** Similarities in the pharmacological modulation of reactive hyperemia and vasodilation to hydrogen peroxide in rat skeletal muscle arterioles: effects of probes for endothelium-derived mediators. *J Pharmacol Exp Ther* 253: 508–512, 1990.
39. **Wu R, Millette E, Wu L, de Champlain J.** Enhanced superoxide anion formation in vascular tissues from spontaneously hypertensive and desoxycorticosterone acetate-salt hypertensive rats. *J Hypertens* 19: 741–748, 2001.
40. **Yada T, Hiramatsu O, Kimura A, Goto M, Ogasawara Y, Tsujioka K, Yamamori S, Ohno K, Hosaka H, Kajiya F.** In vivo observation of subendocardial microvessels of the beating porcine heart using a needle-probe videomicroscope with a CCD camera. *Circ Res* 72: 939–946, 1993.
41. **Yada T, Hiramatsu O, Kimura A, Tachibana H, Chiba Y, Lu S, Goto M, Ogasawara Y, Tsujioka K, Kajiya F.** Direct in vivo observation of subendocardial arteriolar response during reactive hyperemia. *Circ Res* 77: 622–631, 1995.

41a. **Yada T, Shimokawa H, Hiramatsu O, Haruna Y, Morita Y, Kashihara N, Shinozaki Y, Mori H, Goto M, Ogasawara Y, Kajiya F.** Cardioprotective role of endogenous hydrogen peroxide during ischemia-reperfusion injury in canine coronary microcirculation in vivo. *Am J Physiol Heart Circ Physiol* 291: H1138–H1146, 2006.

42. **Yada T, Shimokawa H, Hiramatsu O, Kajita T, Shigeto F, Goto M, Ogasawara Y, Kajiya F.** Hydrogen peroxide, an endogenous endothelium-derived hyperpolarizing factor, plays an important role in coronary autoregulation in vivo. *Circulation* 107: 1040–1045, 2003.
44. **Yada T, Shimokawa H, Hiramatsu O, Shinozaki Y, Mori H, Goto M, Ogasawara Y, Kajiya F.** Important role of endogenous hydrogen peroxide in pacing-induced metabolic coronary vasodilatation in dogs in vivo. *J Am Coll Cardiol* 50: 1272–1278, 2007.
45. **Zhang DX, Gutterman DD.** Mitochondrial reactive oxygen species-mediated signaling in endothelial cells. *Am J Physiol Heart Circ Physiol* 292: H2023–H2031, 2007.

Acta Physiol 2007, 191, 275–284

Characterization of ouabain-induced noradrenaline and acetylcholine release from *in situ* cardiac autonomic nerve endings

T. Yamazaki,[1] T. Akiyama,[1] H. Kitagawa,[1] F. Komaki,[1] H. Mori,[1] T. Kawada,[2] K. Sunagawa[2] and M. Sugimachi[2]

1 Department of Cardiac Physiology, National Cardiovascular Center Research Institute, Suita, Osaka, Japan

2 Department of Cardiovascular Dynamics, National Cardiovascular Center Research Institute, Suita, Osaka, Japan

Received 11 January 2007, revision requested 28 March 2007, revision received 29 May 2007, accepted 30 June 2007
Correspondence: T. Yamazaki, Department of Cardiac Physiology, National Cardiovascular Center Research Institute, 5-7-1 Fujishirodai, Suita, Osaka 565, Japan. E-mail: yamazaki@ri.ncvc.go.jp

Abstract

Aim: Although ouabain modulates autonomic nerve ending function, it is uncertain whether ouabain-induced releasing mechanism differs between *in vivo* sympathetic and parasympathetic nerve endings. Using cardiac dialysis, we examined how ouabain induces neurotransmitter release from autonomic nerve ending.

Methods: Dialysis probe was implanted in left ventricle, and dialysate noradrenaline (NA) or acetylcholine (ACh) levels in the anaesthetized cats were measured as indices of neurotransmitter release from post-ganglionic autonomic nerve endings.

Results: Locally applied ouabain (100 μM) increased in dialysate NA or ACh levels. The ouabain-induced increases in NA levels remained unaffected by cardiac sympathetic denervation and tetrodotoxin (Na^+ channel blocker, TTX), but the ouabain-induced increases in ACh levels were attenuated by TTX. The ouabain-induced increases in NA levels were suppressed by pretreatment with desipramine (NA transport blocker) and augmented by reserpine (vesicle NA transport blocker). In contrast, the ouabain-induced increases in ACh levels remained unaffected by pretreatment with hemicholinium-3 (choline transport blocker) but suppressed by vesamicol (vesicle ACh transport blocker). The ouabain-induced increases in NA levels were suppressed by pretreatment with ω-conotoxin GVIA (N-type Ca^{2+} channel blocker), verapamil (L-type Ca^{2+} channel blocker) and TMB-8 (intracellular Ca^{2+} antagonist). The ouabain-induced increases in ACh levels were suppressed by pretreatment with ω-conotoxin MVIIC (P/Q-type Ca^{2+} channel blocker), and TMB-8.

Conclusions: Ouabain-induced NA release is attributable to the mechanisms of regional exocytosis and/or carrier-mediated outward transport of NA, from stored NA vesicle and/or axoplasma, respectively, while the ouabain-induced ACh release is attributable to the mechanism of exocytosis, which is triggered by regional depolarization. At both sympathetic and parasympathetic nerve endings, the regional exocytosis is because of opening of calcium channels and intracellular calcium mobilization.

Keywords acetylcholine, Ca^{2+} channels, cat, microdialysis, Na^+,K^+-ATPase, noradrenaline.

 doi: 10.1111/j.1748-1716.2007.01749.x

It is generally accepted that ouabain modulates autonomic nerve function by inhibition of membrane Na^+,K^+-ATPase (Gillis & Quest 1979). This neuronal modulatory effect was mainly reported with *in vitro* sympathetic (Sweadner 1985), parasympathetic nerve endings (Satoh & Nakazato 1992, Gomez *et al.* 1996) and adrenal glands (Haass *et al.* 1997). Furthermore, ouabain-induced modulatory effect was reported with *in vitro* studies on motor endplate (Vyskocil & Illes 1977, Zemkova *et al.* 1990). From these *in vitro* studies, several mechanisms are presently suggested to induce release of neurotransmitter from the nerve endings. However, it is uncertain whether the manner of modulation differs between *in vivo* sympathetic and parasympathetic nerve endings. A major concern is whether ouabain induces a brisk increase in neurotransmitter efflux (spontaneous neurotransmitter release). Kranzhöfer *et al.* (1991) reported that ouabain-induced spontaneous noradrenaline (NA) release from sympathetic nerve endings. On the other hand, ouabain-induced spontaneous acetylcholine (ACh) release was reported *in vitro* studies using synaptosomes (Satoh & Nakazato 1992). No reports have described *in vivo* spontaneous ACh release evoked by ouabain. Further, a second issue is at which site ouabain induces neurotransmitter release: stored vesicle or axoplasma (Haass *et al.* 1997). NA and ACh release have been reported in stored vesicles and/or the axoplasma. It is uncertain, however, which site induces the predominant neurotransmitter release evoked by ouabain *in vivo*. Furthermore, the mechanisms underlying the neurotransmitter release evoked by ouabain remain unclear. Neuronal effects of ouabain have been attributed to the inhibitory action upon Na^+,K^+-ATPase and transmembrane sodium pump (Haass *et al.* 1997). As a consequence of the reduced sodium gradient at the plasma membrane, two possible mechanisms have been proposed to induce NA release from nerve endings; (i) carrier-mediated reversed NA transport, and (ii) Ca^{2+}-dependent exocytotic NA release. The manner and mechanisms of NA efflux have been extensively studied and accepted *in vivo* in isolated tissues (Sweadner 1985, Haass *et al.* 1997). However, it remains unclear whether these assumptions are valid in the cardiac sympathetic or parasympathetic nerve endings *in vivo*.

Cardiac dialysis technique in combination with highly sensitive measurement of NA or ACh has offered a powerful method for detecting the low level of dialysate NA or ACh obtained from the myocardial space (Akiyama *et al.* 1991, 1994). We demonstrated that dialysate NA or ACh levels were affected by local administration of pharmacological agents through dialysis probes, indicating that changes in dialysate NA or ACh levels reflect NA or ACh output from cardiac postganglionic sympathetic or parasympathetic nerve endings (Yamazaki *et al.* 1997, Kawada *et al.* 2001) respectively. Using dialysis technique, ouabain can be administered locally and it is possible to monitor NA or ACh output following locally applied ouabain (Yamazaki *et al.* 2001). Furthermore, comparison of the dialysate NA response in the presence and absence of neuronal agents can differentiate carrier-mediated NA release from calcium dependent exocytotic NA release (Yamazaki *et al.* 1997). With locally applied neuronal blockers, we examined the mechanisms and the sites underlying NA or ACh release evoked by ouabain.

Methods

Animal preparation

Adult cats were anaesthetized with pentobarbital sodium (30–35 mg kg^{-1} i.p.). The level of anaesthesia was maintained with a continuous intravenous infusion of pentobarbital sodium (1–2 mg kg^{-1} h^{-1}). The animals were intubated and ventilated with room air mixed with oxygen. Body temperature was maintained using a heated pad and lamp. All protocols were performed in accordance with the National Cardiovascular Center Research Institute Animal Care Ethics Committee guidelines that were in strict compliance with the NIH Guide for the Care and Use of Laboratory Animals. Electrocardiogram and mean arterial pressure were simultaneously monitored with a data recorder. The sixth rib on the left side was resected to expose the heart. With a fine guiding needle, one or two dialysis probes for dialysate sampling were implanted in the mid wall of the anterolateral region of the left ventricle. Heparin (100 U kg^{-1}) was administered after implantation of the dialysis probe and a maintenance dose was given every hour thereafter.

Dialysis technique

The material and properties of the dialysis probe were described previously (Akiyama *et al.* 1991, 1994). Briefly, we designed a transverse dialysis probe. Both ends of a dialysis fibre (13 mm length, 0.31 mm o.d. and 0.2 mm i.d.; PAN-1200, 50 000 molecular weight cutoff, Asahi Chemical, Tokyo, Japan) were connected and glued to polyethylene tubes (25 cm length, 0.5 mm o.d. and 0.2 mm i.d.). The dialysate NA or ACh levels were measured in separate animals. For the measurement of dialysate NA, the dialysis probe was perfused with Ringer's solution at 10 μL min^{-1}. Sampling periods were 2 min in duration (one sample volume = 20 μL), which was the minimum period necessary to collect sufficient NA for satisfactory measurement. For the measurement of dialysate ACh, Ringer's solution containing eserine (choline esterase

 doi: 10.1111/j.1748-1716.2007.01749.x

inhibitor, 100 μM) was perfused at 2 μL min^{-1} and sampling periods were 15 min in duration. Dialysate sampling was started 120 min after probe implantation, when the dialysate NA or ACh concentration had reached a steady level. Each sample was collected in a microtube containing 0.1 N HCl or phosphate buffer to prevent oxidation. The dead-space volume between the dialysis and sample tube was measured. Taking this dead-space into account, samples were obtained.

Experimental protocols

In our previous study, we demonstrated that the dialysate NA or ACh levels reflect cardiac neuronal NA or ACh disposition at the nerve endings (Yamazaki *et al.* 1997, Kawada *et al.* 2001). Therefore, in the present study, we obtained dialysate samples and measured the dialysate NA or ACh levels as an index of NA or ACh output from post-ganglionic sympathetic or parasympathetic nerve endings respectively. Generally two mechanisms and sites are proposed to induce NA and ACh release from nerve endings: exocytotic (quantum) release from the stored vesicle and non-exocytotic (non-quantum) release from the axoplasma. The present studies were designed to clarify whether ouabain-induced NA or ACh efflux are affected by local administration of pharmacological agents that modify experimental conditions.

Protocol 1: Time courses of dialysate NA and ACh levels during local administration of ouabain. We examined the time course of dialysate NA and ACh levels during local administration of ouabain (100 μM). Ouabain was administered for 60 min. Dialysate NA levels were measured before and at 10-min intervals during ouabain administration. Dialysate ACh levels were collected in consecutive 15-min sampling periods.

Protocol 2: Influence of nerve transection and Na^+ channels on dialysate NA or ACh response evoked by ouabain. To test whether ouabain modulated central-mediated exocytotic neurotransmitter release, we examined the time course of ouabain-induced dialysate NA and ACh levels after transection of stellate ganglia or cervical parasympathetic nerve tract. For cardiac sympathetic denervation, the region of the stellate ganglia was exposed through the intercostal space, and bilateral transection of stellate ganglia was performed. After cardiac sympathetic denervation, heart rate response to carotid occlusion was blunted. In separate cats, cervical vagotomy was performed. We started dialysate sampling at 120 min after surgical interruption and ouabain-induced NA or ACh efflux was examined. Furthermore, to examine involvement of deporalization on NA or ACh release, ouabain-induced NA or ACh efflux was measured with addition of tetrodotoxin (TTX, 10 μM) through the dialysis probe. At 60 min after the beginning of TTX administration, we started the control sampling and examined the ouabain-induced NA or ACh response.

Protocol 3: Influence of NA-, ACh- and choline transporters on dialysate NA or ACh response evoked by ouabain. To test whether ouabain-induced neurotransmitter efflux was derived from axoplasma or stored vesicle, ouabain-induced NA or ACh efflux was examined with local administration of pharmacological agents, which affected the transport and content of neurotransmitter at the nerve endings. Membrane carrier-mediated NA transport was blocked by local administration of desipramine, whereas vesicular NA import was blocked by local administration of reserpine. In either case, ouabain-induced NA efflux was examined with the addition of desipramine (100 μM) or reserpine (10 μM) through the dialysis probe. The dosage of agent-administration was decided after referring to the previous studies (Akiyama *et al.* 1994, Yamazaki *et al.* 1997). Membrane carrier-mediated choline transport was blocked by local administration of hemicholinium-3 (10 μM), whereas vesicular ACh import was blocked by local administration of vesamicol (10 μM) (Kawada *et al.* 2001). In either case, ouabain-induced ACh efflux was examined with the addition of hemicholinium-3 or vesamicol through the dialysis probe.

Protocol 4: Influence of Ca^{2+} transporter, channel, mobilization on dialysate NA or ACh response evoked by ouabain. To test the contention that ouabain-induced neurotransmitter efflux was modulated by changes in intracellular Ca^{2+} levels, the influence of Ca^{2+} transporter, channel, mobilization on the dialysate NA or ACh response evoked by ouabain was examined. We focused on the involvement of three types of voltage-dependent Ca^{2+} channel, the L- and N types in the NA release evoked by ouabain. Sixty minutes after starting local administration of verapamil (100 μM), or ω-conotoxin GVIA (10 μM), we measured the ouabain-induced NA response. Second, we examined the involvement of plasma membrane Na^+/Ca^{2+} exchanger in the NA release evoked by ouabain. The inhibitors of membrane Na^+/Ca^{2+} exchange (dechlorobezamil; 100 μM, or KB7943; 10 μM) were locally administered through the dialysis probe and the ouabain-induced NA response was measured. Third, we examined the involvement of intracellular Ca^{2+} level in the NA release evoked by ouabain. An intracellular Ca^{2+} antagonist [3,4,5-trimethoxybenzoic acid 8-(dietyl amino)-octyl ester (TMB-8)] blocks the efflux of calcium from intracellular calcium stores without affecting influx

 doi: 10.1111/j.1748-1716.2007.01749.x

(Wiedenkeller & Sharp 1984). TMB-8 (1 mM) was locally administered through the dialysis probe and ouabain-induced NA response was measured. A similar pharmacological intervention was performed and ouabain-induced ACh responses were measured. Sixty minutes after starting local administration of verapamil (100 μM), or ω-conotoxin GVIA (10 μM), ω-conotoxin MVIIC (10 μM), we measured the ouabain-induced ACh response. The inhibitor of membrane Na^+/Ca^{2+} exchange (KB7943; 10 μM) was locally administered through the dialysis probe and the ouabain-induced ACh response was measured. Third, an intracellular Ca^{2+} antagonist (TMB-8, 1 mM) was locally administered through the dialysis probe and ouabain-induced ACh response was measured.

Analytical procedure

Dialysate NA concentrations were measured by HPLC with electrochemical detection (HPLC-ECD; Eicom, Kyoto, Japan). An alumina procedure was performed to remove the interfering compounds from the dialysate. The detection limit was 50 fmol per injection. Dialysate ACh concentration was measured directly by another HPLC-ECD. The detection limit was 50 fmol per injection. Details of HPLC-ECD for the NA and ACh measurements have been described elsewhere (Akiyama *et al.* 1991, 1994).

At the end of each experiment, the cats were killed with an overdose of pentobarbital sodium, and the implant sites were checked to confirm that the dialysis probes had been implanted within the left ventricular myocardium. Statistical analysis of the data was performed by analysis of variance (ANOVA). Statistical significance was defined as $P < 0.05$. Values are presented as mean ± SE.

Results

Protocol 1: Time course of dialysate NA and ACh levels during local administration of ouabain

Although local administration of ouabain did not affect haemodynamic parameters including heart rate, mean arterial pressure and electrocardiogram, ouabain induced the efflux of NA. Figure 1 (upper panel) shows the time course of the dialysate NA levels during local administration of ouabain (100 μM). Dialysate NA level increased significantly from 0.18 ± 0.06 nmol L^{-1} at control to 2.39 ± 0.53 nmol L^{-1} at 10, 12.92 ± 1.39 nmol L^{-1} at 20 min and 14.79 ± 1.97 nmol L^{-1} at 30 min. Subsequently, a slow decline occurred but high dialysate NA levels were maintained during locally applied ouabain. Peak level of dialysate NA ranged from 20 to 30 min after the beginning of ouabain administration. Figure 1 (lower panel) shows the time course of the dialysate ACh levels during local administration of ouabain (100 μM). Dialysate ACh level increased significantly from 0.91 ± 0.05 nmol at control to 3.6 ± 0.60 nmol L^{-1} at 0–15, 8.1 ± 1.4 nmol L^{-1} at 15–30 min and 6.8 ± 1.25 nmol L^{-1} at 30–45 min. Peak level of dialysate ACh appeared at 15–30 min after the beginning of ouabain administration.

Protocol 2: Influence of denervation and TTX on dialysate NA and ACh responses evoked by ouabain

We sampled the dialysates over 60 min of ouabain administration. To compare ouabain-induced NA or ACh levels under various interventions, ouabain-induced dialysate NA or ACh levels were subtracted from the control values. The sum of relative changes in dialysate NA or ACh (the unit: Σnmol/L) was expressed as an index of total NA or ACh release evoked by ouabain. Figure 2 (upper panel) shows the total NA release evoked by ouabain when cardiac sympathetic nerves were either intact, transected, pretreated with TTX. The ouabain-induced total NA release did not differ among them. Figure 2 (lower panel) shows the total ACh release evoked by ouabain when cardiac parasympathetic nerves were either intact, transected, or pretreated with TTX. The ouabain-induced total ACh release did not differ between the intact cardiac parasympathetic nerve and denervated groups whereas addition of TTX significantly inhibited the total ACh release by approx. 57% of vehicle.

Protocol 3: Influence of transport blocking agents on dialysate NA and ACh responses evoked by ouabain

Figure 3 (upper panel) shows the total NA release evoked by ouabain among various pharmacological interventions. Pretreatment with reserpine caused significant augmentation of the ouabain-induced total NA release whereas pretreatment with desipramine caused significant suppression of the total NA release. Figure 3 (lower panel) shows the total ACh release evoked by ouabain among various pharmacological interventions. The ouabain-induced total ACh release did not differ between the intact and hemicholinium-3 pretreated groups whereas addition of vesamicol significantly inhibited the total ACh release by approx. 45% of vehicle.

Protocol 4: Influence of Ca^{2+} mobilization on dialysate NA and ACh responses evoked by ouabain

Figure 4 (upper panel) shows the total NA release evoked by ouabain among various Ca^{2+} interventions. The total NA release in the 60 min after administration

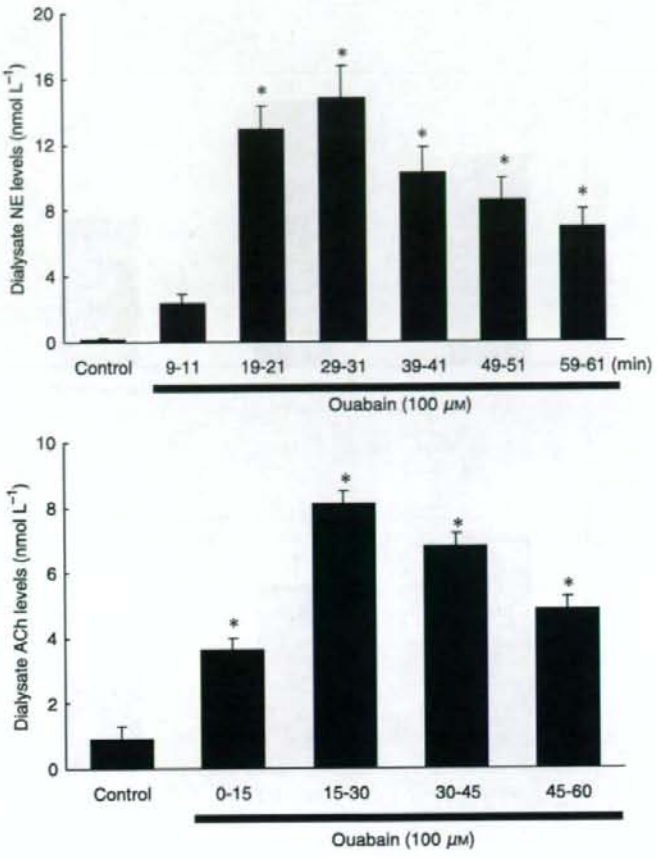

Figure 1 Upper panel: Time course of dialysate noradrenaline (NA) levels during local administration of ouabain (100 μM). Ouabain increased the dialysate NA levels. Subsequently, a slow decline occurred but high NA levels were maintained. Lower panel: Time course of dialysate acetylcholine (ACh) levels during local administration of ouabain (100 μM). Ouabain increased the dialysate ACh levels. Subsequently, a slow decline occurred but high ACh levels were maintained. Values are presented as the mean ± SE (for each column $n = 6$) $^*P < 0.05$ vs. control.

of ouabain was significantly suppressed by approx. 47% and 55% of vehicle by addition of verapamil and ω-conotoxin GVIA. Pretreatment with TMB-8 caused significant suppression of the ouabain-induced total NA release whereas pretreatment with neither KB-7943 nor dechlorobezamil altered the total NA release. Figure 4 (lower panel) shows the total ACh release evoked by ouabain among various Ca^{2+} interventions. The total ACh release in the 60 min after administration of ouabain was significantly suppressed by approx. 57% of vehicle by addition of ω-conotoxin MVIIC. Pretreatment with neither verapamil nor ω-conotoxin GVIA altered the total ACh release. Pretreatment with TMB-8 caused significant suppression of the ouabain-induced total ACh release whereas pretreatment with KB-7943 did not alter the total ACh release.

Discussion

The present study indicates that in an *in vivo* preparation, ouabain alone induced NA or ACh release from sympathetic or parasympathetic nerve endings respectively. This discussion addresses mainly similarities and differences in ouabain alone induced NA or ACh releasing sites and mechanisms.

Regional depolarization evoked by ouabain

At the post-ganglionic nervous endings, ouabain induced NA and ACh release. The transection of sympathetic or parasympathetic nerve did not affect the amount of NA or ACh release evoked by ouabain. After the transection of cardiac sympathetic or parasympathetic nerves, ouabain at 100 μM induced increases in dialysate NA or ACh levels, which were as much as those evoked by electrical stimulation of the autonomic nerve (Akiyama *et al.* 1994, Yamazaki *et al.* 1997). These data suggest that ouabain itself induces regional depolarization following exocytosis. In the case of locally administered ouabain, ouabain produced intracellular Na^+ accumulation evoked by the inhibition of Na^+,K^+-ATPase (Mclvor & Cummings 1987).

 doi: 10.1111/j.1748-1716.2007.01749.x

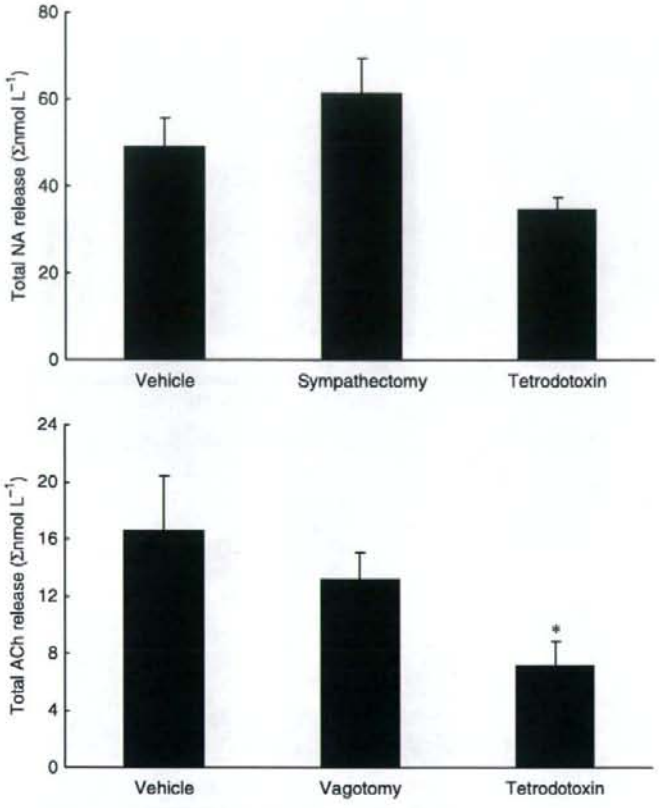

Figure 2 Upper panel: Ouabain-induced dialysate noradrenaline (NA) release in vehicle, cardiac sympathetic denervated and tetrodotoxin pretreated groups. Total NA release evoked by ouabain did not differ among the three groups. Lower panel: Ouabain-induced dialysate acetylcholine (ACh) release in vehicle, cardiac vagal denervated and tetrodotoxin pretreated groups. Total ACh release evoked by ouabain was suppressed by the pretreatment with tetrodotoxin. Values are presented as the mean ± SE (for each column $n = 6$). $^*P < 0.05$ vs. vehicle.

Regional depolarization may occur because of intracellular Na^+ accumulation (Calabresi *et al.* 1999, Dierkes *et al.* 2006). Similar finding was observed on motor endplate (Zemkova *et al.* 1990). Ouabain can increase the spontaneous ACh release by progressive decline in membrane potential when Na^+ pump is inhibited. If regional depolarization does indeed induce ACh or NA release via exocytosis from the stored vesicle, then pretreatment with TTX could inhibit this response. Local administration of TTX markedly inhibits ACh release whereas it only slightly inhibits the NA release evoked by ouabain. These results indicate that ouabain caused regional depolarization and exocytotic ACh release at the parasympathetic nerve endings. This conclusion is consistent with *in vitro* studies reported by Satoh & Nakazato (1992), and raises the question as to why TTX inhibited the ACh release but not the NA release evoked by ouabain. In the case of NA efflux evoked by ouabain, intracellular Na^+ accumulation may lead to a reduction in the Na^+ gradient between the intracellular and extracellular spaces. This reduced Na^+ gradient may cause carrier-mediated outward NA transport from axoplasma (Sharma *et al.* 1980). The threshold for intracellular Na^+ accumulation coupled to carrier-mediated outward NA transport might be lower than that for regional depolarization. Thus Na^+ accumulation coupled to regional depolarization may occur at the parasympathetic nerve endings but not at the sympathetic nerve endings.

The sites of neurotransmitter efflux evoked by ouabain

In general, two possible sites (the stored vesicle and axoplasma) were proposed to derive efflux of neurotransmitter at the nerve endings (Smith 1992, Vizi 1998). In the cholinergic nerve endings, a quantum amount of ACh was released from the stored vesicle via depolarization. Furthermore, a non-quantum amount of ACh seems to be leaked from the axoplasma without ACh transporter (Nikolsky *et al.* 1991). Local administration of vesamicol suppressed the ACh efflux evoked by ouabain. In contrast, local administration of hemicholinium-3 did not affect the ACh efflux evoked by ouabain. These data suggested that the ACh efflux was predominantly derived from the stored vesicle. This finding is consistent with the above-mentioned

Journal compilation © 2007 Scandinavian Physiological Society, doi: 10.1111/j.1748-1716.2007.01749.x

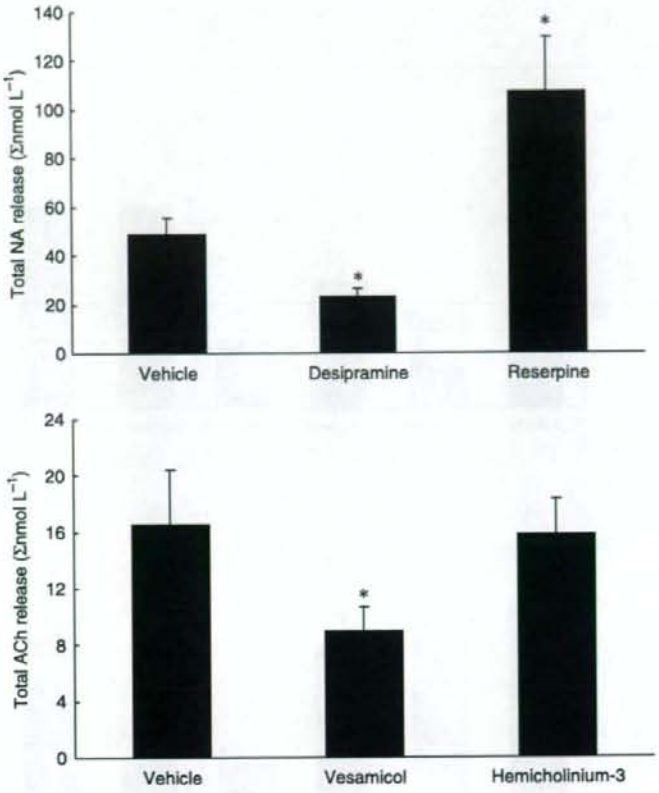

Figure 3 Upper panel: Ouabain-induced dialysate noradrenaline (NA) release among vehicle, desipramine and reserpine pretreated groups. Total NA release evoked by ouabain was suppressed by the pretreatment with desipramine and augmented by that with reserpine. Lower panel: Ouabain-induced dialysate acetylcholine (ACh) release in vehicle, vesamicol and hemicholinium-3 pretreated groups. Total ACh release evoked by ouabain was suppressed by the pretreatment with vesamicol. Values are presented as the mean ± SE (for each column $n = 6$). $^*P < 0.05$ vs. vehicle.

mechanism. Our data did not rule out the possibility of ACh efflux from the axoplasma. Vesamicol lowered the non-quantum ACh release by blocking the incorporated vesicle transporter in the terminal membrane (Edward *et al.* 1985). This involvement seems to be smaller than the involvement of ACh efflux from the stored vesicle.

Previous studies suggested that two different mechanisms (exocytosis and carrier-mediated outward transport) contributed to the amount of NA efflux evoked by ouabain (Kranzhöfer *et al.* 1991, Haass *et al.* 1997). The exocytotic NA release derived from the stored vesicle, whereas NA transporter carried out NA from the axoplasmic site via a reduced Na^+ gradient. However, it is uncertain which mechanism is predominantly involved in ouabain-induced NA efflux. To examine which site predominantly induced the neurotransmitter efflux evoked by ouabain, we administered vesicle and membranous amine transport blockers, which affected the neurotransmitter efflux evoked by ouabain. If NA efflux predominantly derives from the axoplasmic site, reserpine could increase axoplasmic NA level and augment the outward NA transport evoked by ouabain. Furthermore, as desipramine impairs carrier-mediated NA transport in both directions, desipramine could block NA efflux. NA release evoked by ouabain was augmented by local administration of reserpine but suppressed by desipramine. These data support the contention that ouabain-induced NA efflux is predominantly derived from the axoplasmic site.

Involvement of Ca^{2+} on ouabain-induced neurotransmitter efflux

Most *in vitro* studies suggested that ouabain somehow increases intracellular Ca^{2+} levels at the nerve endings and synaptosomes (Katsuragi *et al.* 1994, Casali *et al.* 1995, Wasserstrom & Aistrup 2005). Ouabain-induced intracellular Na^+ accumulation could evoke an elevation of intracellular Ca^{2+} level via Ca^{2+} channel opening (Katsuragi *et al.* 1994), Ca^{2+} release from internal stores (Nishio *et al.* 2004), and/or Na^+/Ca^{2+} exchange (Verbny *et al.* 2002). Thus, the elevation of intracellular Ca^{2+} may be associated with NA or ACh release from the autonomic nerve endings. At the parasympathetic nerve endings, neither verapamil nor ω-conotoxin GVIA

 doi: 10.1111/j.1748-1716.2007.01749.x

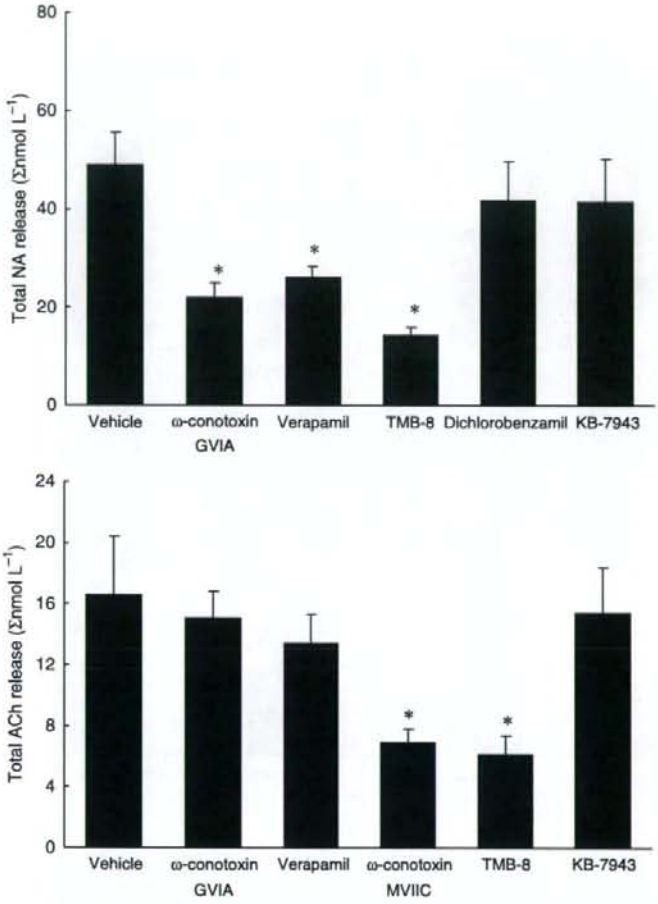

Figure 4 Upper panel: Ouabain-induced dialysate noradrenaline (NA) release in various Ca^{2+} interventions. Total NA release evoked by ouabain was suppressed by the pretreatment with ω-conotoxin GVIA, verapamil, TMB-8. Lower panel: Ouabain-induced dialysate acetylcholine (ACh) release in various Ca^{2+} interventions. Total ACh release evoked by ouabain was suppressed by the pretreatment with ω-conotoxin MVIICA or TMB-8. Values are presented as the mean ± SE (for each column $n = 6$). $^*P < 0.05$ vs. vehicle.

affected ACh release but ω-conotoxin MVIIC inhibited ACh release evoked by ouabain. Furthermore, KB-7943 did not affect either the ACh release evoked by ouabain. These data suggest that N or L-type Ca^{2+} channels or reversal Na^+/Ca^{2+} exchange might not be responsible for the ACh release evoked by ouabain. However, a marked suppression of ouabain-induced ACh release was observed with the addition of P/Q types channel blocker or TMB-8. In the case of parasympathetic nerve endings, Ca^{2+} elevation coupled to ACh release might be derived via internal stores or Ca^{2+} channels (P/Q types) rather than Na^+/Ca^{2+} exchange (Casali *et al.* 1995, Kawada *et al.* (in press)).

In the case of NA, ω-conotoxin GVIA or verapamil suppressed the NA release evoked by ouabain. Ouabain-induced NA release was independent of depolarization (TTX-resistant) but associated with the opening of Ca^{2+} channel. Furthermore, neither KB-7493 nor dichlorobenzamil affected the NA release evoked by ouabain. These data suggest that bi-directions of Na^+/Ca^{2+} exchange might not be responsible for the elevation of intracellular Ca^{2+} levels evoked by ouabain. A marked suppression of ouabain-induced NA release was observed with the addition of TMB-8. Taking these findings together, in the case of sympathetic nerve endings, Ca^{2+} elevation coupled to NA release might be derived via Ca^{2+} channels or internal store rather than membrane Na/Ca^{2+} exchange.

Although the type of Ca^{2+} channel for the NA or ACh release differed, involvement of cytosol Ca^{2+} in ouabain-induced neurotransmitter release did not differ between the parasympathetic and sympathetic nerve endings. However, the relation between TTX sensitive Na^+ channel and Ca^{2+} channel opening may differ between the parasympathetic and sympathetic nerve endings. In the present study, ouabain-induced NA efflux was suppressed by ω-conotoxin GVIA but not by TTX, indicating that TTX sensitive depolarization was not involved in Ca^{2+} channel opening coupled to exocytotic NA release. In contrast to NA release,

Journal compilation © 2007 Scandinavian Physiological Society, doi: 10.1111/j.1748-1716.2007.01749.x

ouabain-induced ACh release was suppressed by TTX and ω-conotoxin MVIIC, indicating that ouabain-induced depolarization and subsequently ACh release via P/Q type Ca^{2+} channel opening. TTX sensitive or resistant response may be interpreted as two different types of neurotransmitter release mechanisms. Alternatively, ouabain may have induced increases in intraneuronal Na^+ accumulation and elevation of extraneuronal K^+ levels by inhibition of Na^+,K^+-ATPase (D'Ambrosio *et al.* 2002). Elevations of both intracellular Na^+ and extracellular K^+ exerted regional depolarization following exocytosis via different mechanisms. In the previous study, we demonstrated that high K^+-induced NA release was insensitive to TTX but sensitive to ω-conotoxin GVIA. Furthermore, high K^+ caused a marked increase in dialysate NA but little increase in dialysate Ach (Yamazaki *et al.* 1998, Kawada *et al.* 2001). Thus high K^+-induced neurotransmitter release might greatly contribute to the increase in dialysate NA evoked by ouabain but might contribute little to the increase in dialysate ACh.

In conclusion, ouabain alone causes a brisk efflux of NA and ACh from cardiac sympathetic and parasympathetic nerve endings respectively. The ouabain-induced ACh release contributes to the mechanism of ACh exocytosis, which is triggered by centrally mediated or regional depolarization. The regional exocytosis is caused by opening of P/Q type Ca^{2+} channels and/or intracellular Ca^{2+} mobilization from the stored ACh vesicle. The ouabain-induced NA release contributes to the mechanisms of regional exocytosis and/or carrier-mediated outward transport of NA, from stored NA vesicle and/or axoplasma respectively. The regional exocytosis is caused by opening of N type Ca^{2+} channels and intracellular Ca^{2+} mobilization.

Conflict of interest

None.

This work was supported by Grants-in-Aid for scientific research (17591659) from the Ministry of Education, Culture, Sports, Science and Technology.

References

Akiyama, T., Yamazaki, T. & Ninomiya, I. 1991. *In vivo* monitoring of myocardial interstitial norepinephrine by dialysis technique. *Am J Physiol* **261**, H1643–H1647.

Akiyama, T., Yamazaki, T. & Ninomiya, I. 1994. *In vivo* detection of endogenous acetylcholine release in cat ventricles. *Am J Physiol* **266**, H854–H860.

Calabresi, P., Marfia, G.A., Centonze, D., Pisani, A. & Bernardi, G. 1999. Sodium influx plays a major role in the membrane depolarization induced by oxygen and glucose deprivation in rat striatal spiny neurons. *Stroke* **30**, 171–190.

Casali, T.A., Gomez, R.S., Moraes-Santos, T. & Gomez, M.V. 1995. Differential effects of calcium channel antagonists on tityustoxin and ouabain-induced release of [3H] acetylcholine from brain cortical slices. *Neuropharmacology* **34**, 599–603.

D'Ambrosio, R., Gordon, D.S. & Winn, H.R. 2002. Differential role of KIR channel and Na(+)/K(+)-pump in the regulation of extracellular K(+) in rat hippocampus. *J Neurophysiol* **87**, 87–102.

Dierkes, P.W., Wusten, H.J., Klees, G., Muller, A. & Hochstrate, P. 2006. Ionic mechanism of ouabian-induced swelling of leech Retzius neurons. *Pflugers Arch* **452**, 25–35.

Edward, C., Dolezal, D., Tucek, S., Zemkova, H. & Vyskocil, F. 1985. Is an acetylcholine transport system responsible for nonquantal release of acetycholine at the rodent myoneural junction? *Proc Natl Acad Sci USA* **82**, 3514–3518.

Gillis, R.A. & Quest, J.A. 1979. The role of the nervous system in the cardiovascular effects of digitalis. *Pharmacol Rev* **31**, 19–97.

Gomez, R.S., Gomez, M.V. & Prado, M.A.M. 1996. Inhibition of Na^+, K^+-ATPase by ouabain opens calcium channels coupled to acetylcholine release in guinea pig myenteric plexus. *J Neurochem* **66**, 1440–1447.

Haass, M., Serf, C., Gerber, S.H. *et al.* 1997. W. Dual effect of digitalis glycoside on norepinephrine release from human atrial tissue and bovine adrenal chromaffin cells: differential dependence on $[Na+]_i$ and $[Ca2+]_i$. *J Mol Cell Cardiol* **29**, 1615–1627.

Katsuragi, T., Ogawa, S. & Furukawa, T. 1994. Contribution of intra-and extracellular Ca^{2+} to noradrenaline exocytosis induced by ouabain and monesin from guinea-pig vas deferens. *Br J Pharmacol* **113**, 795–800.

Kawada, T., Yamazaki, T., Akiyama, T. *et al.* 2006. Effects of Ca2+ channel anatagonists on nerve stimulation-induced and ischemia-induced myocardial interstitial acetylcholine release in cats. *Am J Physiol* **291**, H2181–2191.

Kawada, T., Yamazaki, T., Akiyama, T. *et al.* 2001. *In vivo* assessment of acetylcholine-releasing function at cardiac vagal nerve terminals. *Am J Physiol* **281**, H139–H145.

Kranzhöfer, R., Haass, M., Kurz, T., Richardt, G. & Schömig, A. 1991. Effect of digitalis glycosides on norepinephrine release in the heart: dual mechanism of action. *Circ Res* **68**, 1628–1637.

McIvor, M.E. & Cummings, C.C. 1987. Sodium fluoride produces a K+ efflux by increasing intracellular Ca2+ through Na+-Ca2+ exchange. *Toxicol Lett* **38**, 169–176.

Nikolsky, E.E., Voronin, V.A. & Vyskocil, F. 1991. Kinetic differences in the effect of calcium on quantal and non-quantal acetylcholine release at the murine diaphragm. *Neurosci Lett* **123**, 192–194.

Nishio, M., Ruch, S.W., Kelly, J.E., Aistrup, G.L., Sheehan, K. & Wasserstrom, J.A. 2004. Ouabain increases sarcoplasmic reticulum calcium release in cardiac myocytes. *J Pharmacol Exp Ther* **308**, 1181–1190.

Satoh, E. & Nakazato, Y. 1992. On the mechanisim of ouabain-induced release of acetylcholine from synaptsomes. *J Neurochem* **58**, 1038–1044.

Sharma, V.K., Pottick, L.A. & Banerjee, S.P. 1980. Ouabain stimulation of noradrenaline transport in guinea pig heart. *Nature* **286**, 817–819.

 doi: 10.1111/j.1748-1716.2007.01749.x

Smith, D.O. 1992. Routes of actylcholine leakage from cytosolic and vesicular compartments of rat motor nerve terminals. *Neurosci Lett* **135**, 5–9.

Sweadner, K. 1985. Ouabain-evoked norepinephrine release from intact rat sympathetic neurons: evidence for carrier-mediated release. *J Neurosci* **5**, 2397–2406.

Verbny, Y., Zhang, C.L. & Chiu, S.Y. 2002. Coupling of calcium homeostasis to axonal sodium in axons of mouse optic nerve. *J Neurophysiol* **88**, 802–816.

Vizi, E.S. 1998. Differential temperature dependence of carrier-mediated (cytoplasmic) and stimulus-evoked (exocytotic) release of transmitter: a simple method to separate two types of relase. *Neurochem Int* **33**, 359–366.

Vyskocil, F. & Illes, P. 1977. Non-quantal release of transmitter at mouse neuromuscular junction and its dependency on the activity of Na^+-K^+ ATPase. *Pflugers Arch* **370**, 295–297.

Wasserstrom, J.A. & Aistrup, G.L. 2005. Digitalis: new actions for an old drug. *Am J Physiol Heart Circ Physiol* **289**, H1781–H1793.

Wiedenkeller, D.E. & Sharp, G.W. 1984. Unexpected potentiation of insulin release by the calcium store blocker TMB-8. *Endocrinolgy* **114**, 116–119.

Yamazaki, T., Akiyama, T., Kitagawa, H., Takauchi, Y., Kawada, T. & Sunagawa, K. 1997. A new, concise dialysis approach to assessment of cardiac sympathetic nerve terminal abnormalities. *Am J Physiol* **272**, H1182–H1187.

Yamazaki, T., Akiyama, T., Kawada, T. *et al.* 1998. Norepinephrine efflux evoked by potassium chloride in cat sympathetic nerves: dual mechanism of action. *Brain Res* **794**, 146–150.

Yamazaki, T., Akiyama, T. & Mori, H. 2001. Effects of nociceptin on cardiac norepinephrine and acetylcholine release evoked by ouabain. *Brain Res* **904**, 153–156.

Zemkova, H., Vyskocil, F. & Edwards, C. 1990. The effect of nerve terminal activity on non-quantal release of acetylcholine at the mouse neuromuscular junction. *J Physiol* **423**, 631–640.

Polymer Journal, Vol. 39, No. 10, pp. 1065–1070 (2007)

Synthesis of Sugar-Polysiloxane Hybrids Having Rigid Main-Chains and Formation of their Nano Aggregates

Koutarou BEPPU,[1] Yoshiro KANEKO,[1] Jun-ichi KADOKAWA,[1,†]
Hidezo MORI,[2] and Takehiro NISHIKAWA[2]

[1]*Department of Nano-structured & Advanced Materials, Graduate School of Science and Engineering, Kagoshima University, 1-21-40 Korimoto, Kagoshima 890-0065, Japan*
[2]*National Cardiovascular Center Research Institute, 5-7-1, Fujishirodai, Suita 565-8565, Japan*

(Received March 22, 2007; Accepted July 12, 2007; Published August 28, 2007)

ABSTRACT: We synthesized sugar-polysiloxane hybrids having rigid main-chains by reaction of sugar-lactones with amine-functionalized polysiloxane (**1**). Reaction of gluconolactone (**2**) with **1** was performed to obtain polysiloxane (**3**) having polyol moieties derived from glucose. This material has the regularly controlled higher-ordered structure in solid state such as the hexagonal phase. A hydrophilic sugar-polysiloxane hybrid (**5**) was prepared by reaction of lactobionolactone (**4**) with **1**. Furthermore, an amphiphilic sugar-polysiloxane hybrid (**8**) was synthesized by introduction of stearoyl groups in addition to sugar groups on the surface of **1**. The SEM image of the amphiphilic material **8** exhibited formation of nano aggregates having the particle diameters of *ca.* 50 nm in water.
[doi:10.1295/polymj.PJ2006268]
KEY WORDS Glycopolymer / Sugar-lactone / Polysiloxane / Amphiphilic / Hybrid / Nano Aggregate /

There has been a growing interest in sugar portions of the glycoproteins because of exhibiting to bind to carbohydrate-recognition proteins, toxins, viruses, and cells. It has been known that a molecular assembly formed from the sugar-residues in the living system expresses stronger recognition ability than that of a single sugar molecule. This, so-called multivalent or cluster effect, has become a principle in the design of artificial glycoconjugate ligands. Therefore, polymeric materials having such functional sugar-residues, *i.e.*, 'glycopolymer', have widely been investigated because these materials efficiently show the multivalent effect.[1] So far, a number of such glycopolymers have been synthesized, which are composed of various organic polymer main-chains combined with a variety of sugar side-chains.[2–6]

Inorganic polymers such as polysiloxanes have various of interesting properties, *e.g.*, high oxygen permeability, low toxicity, and biocompatibility, which are advantages as biomaterials. Therefore, sugar-polysiloxane hybrids would be expected to have a significant potential for biological applications. In previous study, synthesis of such sugar-inorganic hybrids, composed of polydimethylsiloxane main-chain has been reported.[7–10] Since the main-chain has relatively flexible nature, nanostructures of the hybrid materials have not been controlled well.

Based on the above viewpoints, we paid attention to amine-functionalized polysiloxanes[11,12] for the main-chain of new sugar-polysiloxane hybrids, which were prepared by sol-gel reaction of amine-functionalized organoalkoxysilanes in strong acid aqueous solutions. The materials have rigid structures and construct hexagonal phase in solid state, because their frameworks are Si-O-Si network structures derived from trifunctional organoalkoxysilane. Furthermore, the materials are soluble in water and have reactive amino groups on the surface. Their rigidity, solubility, and reactivity would be advantageous properties to controlling nanostructures and introduction of various functional groups on the surface, in addition to the general characteristics of the inorganic polymers.

In previous communication, we briefly reported simple preparation method for a rigid polysiloxane hybrid (**3**) having polyol moieties using the amine-functionalized polysiloxane (**1**) and gluconolactone (**2**) (Scheme 1).[13] Because the sugar lactones like **2** react with the amino groups without protection of the hydroxy groups, they are useful substrates for such the simple procedure to exclude multi-reaction steps. However, **2** was not suitable for preparation of materials containing the sugar substituents, because the ring-opened moieties like the side chain of **3** formed from **2** had no any sugar-residues. Therefore, we have been carrying out studies on the synthesis of sugar-functionalized polysiloxane hybrids using disaccharide-lactone such as lactobionolactone (**4**), because the existence of sugar-residues can be maintained in spite of opening the lactone ring of **4** by the reaction with **1**.

†To whom correspondence should be addressed (Tel: +81-99-285-7743, Fax: +81-99-285-3253, E-mail: kadokawa@eng.kagoshima-u.ac.jp).

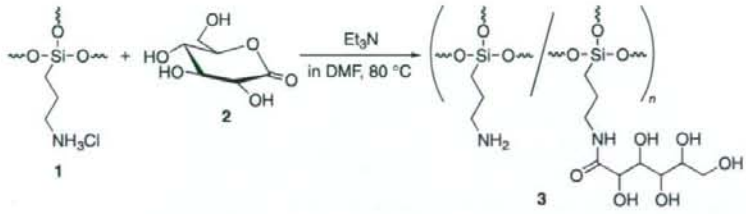

Scheme 1.

In this paper, we describe the synthesis of sugar-polysiloxane hybrids having rigid main-chains by the reaction of sugar-lactones with **1**. Furthermore, we prepared an amphiphilic sugar-polysiloxane hybrid by introduction of long alkyl chains in addition to sugar-residues on the surface of **1** to promote the formation of the nano aggregates in water, expecting the multivalent effects.

EXPERIMENTAL

Materials

The polysiloxane **1** was prepared according to the literature procedure.[11] *N,N*-Dimethylformamide (DMF), dimethyl sulfoxide (DMSO), and triethylamine were purified by distillation. Other reagents were used as received.

*Reaction of **1** with Gluconolactone **2***[13]

To a suspension of **1** (0.147 g, 1.0 mmol unit) in DMF (2.5 mL) was successively added triethylamine (0.15 mL, 1.1 mmol) and a solution of **2** (0.891 g, 5.0 mmol) in DMF (10 mL) with vigorously stirring at 80 °C under argon. After the mixture was stirred further at that temperature for 13 h, the obtained product was isolated by filtration, washed with DMF and acetone, and then dried under reduced pressure at 40 °C to yield 0.191 g of the yellow-powdered **3**. ^{1}H NMR (600 MHz, D_2O): δ 4.38–4.26 (br, -C(=O)-C*H*-), δ 4.16–4.05 (br, -C(=O)CH(OH)C*H*-), δ 3.88–3.60 (br, -C*H*(OH)C*H*(OH)CH_2-), δ 3.41–3.10 and 3.06–2.91 (br, -NCH_2-), δ 1.88–1.45 (br, -NCH$_2$CH_2-CH$_2$Si-), δ 0.94–0.47 (br, -CH_2Si-).

*Synthesis of Hydrophilic Sugar-Polysiloxane Hybrid (**5**)*

To a suspension of **1** (0.147 g, 1.0 mmol unit) in DMSO (3.0 mL) was successively added triethylamine (0.34 mL, 2.4 mmol) and a solution of **4** (1.701 g, 5.0 mmol) in DMSO (10 mL) with vigorously stirring at 80 °C under argon, and the mixture was stirred further at that temperature for 2 h. The mixture became gradually homogeneous solution. The solution was poured into acetone (300 mL) to precipitate the powdered product. The precipitated product was isolated by filtration, successively washed with acetone, hydrochloric acid (HCl) methanol solution and methanol, and then dried under reduced pressure at 40 °C to yield 0.332 g of the light yellow-powdered **5**. ^{1}H NMR (600 MHz, D_2O): δ 4.65–4.50 (br, -OC*H*-(CH-)O-), δ 4.50–4.32 (br, -C(=O)C*H*(OH)-), δ 4.32–4.13 (br, -C(=O)CH(OH)C*H*(OH)-), δ 4.08–3.49 (br, -C*H*(O-)C*H*(OH)CH_2OH, -C*H*(OH)C*H*(OH)C*H*(OH)-C*H*(O-)CH_2OH), δ 3.40–3.12 (br, -C(=O)NHCH_2-), δ 3.12–2.87 (br, Cl·NH$_3$CH_2-), δ 1.95–1.43 (br, -NCH$_2$CH_2CH$_2$Si-), δ 0.93–0.50 (br, -CH_2Si-).

*Synthesis of Stearoyl-Carrying Polysiloxane (**7**)*

To a solution of **1** (0.440 g, 3.0 mmol unit) in water (10 mL) was successively added triethylamine (1.0 mL, 7.2 mmol) and a solution of stearoyl chloride (**6**) (0.182 g, 0.6 mmol) in DMF (30 mL) with vigorously stirring at room temperature, and the solution was stirred further at that temperature for 10 min. After 5 mol/L HCl aqueous solution (2.88 mL, 14.4 mmol) was added to this mixture and this solution was stirred further for 5 min, the solution was poured into acetone (300 mL) to precipitate the powdered product. The precipitated product was isolated by filtration, washed with acetone and chloroform, and then dried under reduced pressure at 40 °C to yield 0.437 g of the white-powdered **7**. ^{1}H NMR (600 MHz, DMSO-d_6-D_2O): δ 3.09–2.72 (br, -NCH_2-), δ 2.20–2.01 (br, -C(=O)CH_2-), δ 1.88–1.55 (br, -NCH$_2$CH_2-CH$_2$Si-), δ 1.50–1.40 (br, -C(=O)CH$_2$CH_2-), δ 1.28–1.10 (br, -CCH_2C-), δ 0.95–0.45 (br, -CH$_3$, -CH_2Si-).

*Synthesis of Amphiphilic Sugar-Polysiloxane Hybrid (**8**)*

To a solution of **7** (0.150 g, 1.3 mmol unit) in DMSO (5 mL) was successively added triethylamine (0.46 mL, 3.3 mmol) and a solution of **4** (2.212 g, 6.5 mmol) in DMSO (15 mL) with stirring at 80 °C, and the solution was stirred further at that temperature for 2 h. The solution was poured into acetone (300 mL) to precipitate the powdered product. The precipitated product was isolated by filtration, successively washed with acetone, HCl methanol solution and